



# Climatology of Snow Depth and Water Equivalent measurements in the Italian Alps (1967 - 2020)

Roberto Ranzi<sup>1</sup>, Paolo Colosio<sup>1</sup>, Giorgio Galeati<sup>2</sup>

<sup>1</sup> Department of Civil, Environmental, Architectural Engineering, and Mathematics, University of Brescia, Brescia 25121, Italy

<sup>2</sup> Italian Hydrological Society, Bologna 40127, Italy

Correspondence to: Paolo Colosio (paolo.colosio1@unibs.it)

**Abstract.** A climatology of SWE based on data collected at 299 gauging sites was performed for the Italian Alps over the 1967 – 2020 period, when the Italian National Electric board conducted routinely and with homogeneous methods snow depth and density measurements. Six hydrological sub-regions were investigated spanning from the eastern Alps to the western Alps at altitudes ranging from 1000 m to 3000 m asl. Measures were conducted at fixed dates at the beginning of each month from 1 February to 1 June and on 15 April. To our knowledge this is the most comprehensive and homogeneous dataset of measured snow depth and density for the Italian Alps. Significant decreasing trends over the years at fixed dates and elevation classes were identified for both snow depth ( $-0.12$  m decade<sup>-1</sup> on average) and snow water equivalent ( $-37$  mm decade<sup>-1</sup> on average) in most of the six investigated areas. The analysis of bulk snow density data showed a temporal evolution along the snow accumulation and melt season, but no altitudinal trends were found. A Moving Average and Running Trend Analysis (MARTA triangles), combined with a Pettitt's test change-point detection, highlighted a decreasing change of snow climatology occurring around the end of the 1980s. Correlation with climatic indexes indicate significant negative values of Pearson correlation coefficient with winter North Atlantic Oscillation (NAO) and positive values with winter West Mediterranean oscillation (WeMO) for some areas and elevation classes. Results of this climatology are synthesized in a temporal polynomial model useful for climatological studies and water resources management in mountain areas.

## 1 Introduction

The effects of global climate change on the cryosphere at different latitudes have been widely studied in the last decades (Pörtner et al., 2019). The comparison between photos of the past decades with the current ones, together with imagery analysis from satellites, confirms the retreat of glaciers in the Alpine region (Ranzi et al., 1999; Beniston, 2012). Analysis of long term observed snow depth and simulated bulk snow density in 20 gauging sites in the Italian Alps highlights a decrease of snow water equivalent especially after the 1990s (Colombo et al., 2022). Modifications of the Greater Alpine Region climate have been confirmed by the analysis of the HISTALP dataset, with significant trends in temperature, twice as the



30 global average, precipitation and relative humidity (Auer et al., 2007; Brunetti et al., 2009). In fact, the alpine region is an extremely sensitive area to the variations of climate condition, making mountain glaciers sentinels of climate change.

Snow is the largest component of the cryosphere in terms of areal extension. Its importance in the Alpine region is related to climatological, hydrological, biological, economic, and social aspects (Beniston et al., 2018). Snow cover regulates the surface energy balance, affecting circulation patterns and atmospheric flow regimes (Ge and Gong, 2009). The hydrological  
35 cycle is strongly dependent on the separation between solid and liquid precipitation and the timing of the melting season onset, mainly driven by temperature, and the hydrological response of high-mountain catchments is often regulated by snowmelt and accumulation (Penna et al., 2016). Moreover, snow accumulation and melting are a major component of the mass balance of glaciers. Snow monitoring is crucial in order to provide a proper estimate of glaciers mass and energy  
40 balance to evaluate glacial response to snow cover variations. The presence of snow is also of paramount importance for ski resorts and for winter tourism in general in the Alpine region, accounting for about 10 billion euro, maintaining seasonal jobs and slowing down the rural depopulation in the valleys (Lehr et al., 2012; Reynard, 2020). The water stored as snow in winter is released as the melting season begins, contributing to the water availability for agriculture and energy production in hydropower plants (HPP).

Hence, it is of great interest for HPP managers having an accurate quantification of the snow water equivalent (SWE) and  
45 possible variability in a climate change scenario (Schaeffli et al., 2007). In view of this, since 1966, ENEL (Italian National Electric Board) conducts systematic observations of snowpack depth and density in the basins subtended by seasonal regulation reservoirs. The ENEL measurement program is similar to other institutional measurement networks (e.g. SNOTEL; Serreze et al., 1999). Before the creation of ENEL, some power companies already took care of periodic measurements of the snowpack consistency on the Alpine and Apennines basins supplying reservoirs within their  
50 competence. However, these surveys were carried out unevenly, adopting different instruments and, of course, with different procedures for processing and interpreting the collected dataset. The ENEL measurement campaigns are scheduled since the early 1960s at fixed dates from the 1st of February to the 1st of June at fixed locations in the catchments of the main Alpine reservoirs. Such extensive and standardized monitoring campaign represents a rich and valuable source of in situ measurements covering a wide portion of the Italian Alps for a 54-years time window spanning the 1967-2020 period.  
55 Hydrological models and remote sensing techniques have been widely used to estimate SWE (Taschner et al., 2004; Tedesco et al., 2015) and snow cover (Terzago et al., 2010). However, in situ measurements are required to validate such estimates and it is not trivial to reconstruct a coherent timeseries long enough to be suitable for climatological studies by means of satellite observations. Lejeune et al. (2019) used snow dataset of 57 years from a mountain meteorological station to evaluate snow depth variability between 1960 and 2017, a temporal range sufficiently wide to evaluate climate impacts on snow  
60 depth. A similar dataset has been used by López-Moreno (2020) to evaluate long-term trends of snow depth and snow cover in the Pyrenees. Schöner et al. (2019) used an ensemble of 196 stations to study the snow depth and its linkages to climate change over the Swiss-Austrian Alps over the monitoring period 1961-2012. A more comprehensive study of the Northern Hemisphere has been carried out by Pulliainen et al. (2019) using the GlobSnow v3.0 dataset (Takala et al., 2011) for the



65 monitoring period 1980-2018. Valt and Cianfarra (2010) found a reduction of snow cover duration and snowfall between  
1950 and 2009, together with breakpoints of the timeseries at the end of the 1980s. Marty et al. (2017) observed a SWE  
decrease, more pronounced in spring than in winter, over the observation period 1968-2012. Colombo et al. (2022) modelled  
the SWE from 19 historical snow depth measurements and studied the links of the Standardized SWE Index with  
teleconnection indexes and temperature anomalies. Marcolini et al. (2017) analysed snow depth series in the Adige basin,  
finding a reduction of snow cover duration and snow depth over the period 1980-2009, especially at low elevation sites. The  
70 dataset we use here covers almost the same period of previous studies, but it is spatial distributed over the Italian Alpine  
Region and includes bulk snow density measurements to estimate SWE. Such combination of spatial and temporal coverage  
makes this dataset an extremely precious support to understand snow variability and climate change impacts in the Italian  
Alps.

In this study, we present a detailed long-term trends and variability analysis of snow depth and SWE measurements in a wide  
75 portion of the Italian Alps between 1967 and 2020. In Section 2, after a description of the study area and the snow depth and  
density measurement procedure, we present the datasets adopted and describe the statistical methodology used for the  
climatological analysis. We also present a simple model to estimate the SWE as function of elevation and day of the year  
based on polynomial regressions of the observed snow depth and bulk snow density. In Section 3 we present and discuss the  
results obtained for snow depth and bulk snow density comparing them with the analysis of meteorological variables and  
80 climatic teleconnection indexes.

## 2 Datasets and methods

### 2.1 The study area and basins aggregation

In this study we focus our analysis on the following basins of the Alpine Region: Cordevole and Piave, in the Veneto  
Region, Cismon, Brenta, Noce, Sarca, Chiese, Valsura, in the Trentino-Alto Adige Region, Mallero, Adda, Bitto, Serio,  
85 Brembo, Oglio, in the Lombardia Region and Toce in the Piemonte Region. We aggregate the individual basins in six groups  
(Figure 1) according to the hydrographic criteria, merging tributaries to the main river branch (e.g. Cordevole aggregated to  
Piave), and the geomorphoclimatic criteria, aggregating basins with similar annual average precipitation, temperature and  
geographical orientation (e.g. Piave and Brenta or Oglio, Chiese and Sarca). Measurements aggregation is a crucial step in  
the analysis and imply the change of scale (Blöschl, 1999). However, we believe that the data aggregation adopted can be  
90 representative of the selected macro-basins.

Toce basin's slopes are mainly east oriented, and its climate is affected by the influence of Lake Maggiore. As it is the only  
basin where data are available in the Piemonte Region, we decided not to aggregate it with other basins (we denote the group  
simply as Toce). Since Serio and Brembo are the tributaries of the lower Adda, downstream Lake Como, and their slope is  
mainly oriented southward, facing Po River valley, they can be grouped in a unique macro-basin denoted as Serio-Brembo.  
95 Bitto and Mallero slopes are respectively North and South facing and both basins are tributaries of the upper Adda, oriented



westward, upstream the Lake Como. Consequently, we aggregate Bitto, Mallero and Adda basins into one group (denoted as Adda). Oglio, Chiese and Sarca basins are fed by meltwater of the Adamello glacier; accordingly, we considered a unique macro basin called Oglio-Chiese-Sarca. We denote as Adige the macro-basin including its tributaries Noce and Valsura. Finally, we aggregate Piave, Brenta, Cisonon and Cordevole in another group (denoted Piave-Brenta), most influenced by the Adriatic Sea.

## 2.2 Snow depth, snow density and snow water equivalent

We use a dataset of snow depth and bulk snow density measurements collected between 1967 and 2020. The locations of the 299 measurement stations, reported in Figure 1, are fixed with minor displacements over the monitoring period. For each measurement station multiple measurements of snow depth were taken and then averaged. The choice of such locations is based on accessibility in every moment of the winter under normal meteorological conditions and representativeness of natural snow deposition, avoiding areas where avalanche snow might be collected or places where other forcings might change the snowpack height. The measurement dates are fixed in time on 1 February, 1 March, 1 April, 15 April, 1 May and 1 June, providing strong consistency for the timeseries analysis.

The tools adopted for height and density measurements of the snowpack have been designed by the Hydrographic Office of the Water Authority of Venice. One of the tools is a snow weighter CN2 type (Figure 2a), derived from the CN1 type, tested by the Snow Commission of the Glaciological committee, through small technical changes suggested by ENEL in order to make the use of it easier and faster. The CN2 type snow weighter is made of four tubular elements in duraluminium, each 50 cm long and with internal diameter of 7.2 cm. Screwable brass caps are attached to the ends of the four tubes, allowing to join two or more elements. On the side of each tube there are measurement notches from 0 to 50 cm in order to measure the exact height of the snow. The checking of this height is completed with a graduated rod, made of three pluggable elements in rust-proof alloy. Other accessories that complete the snow weighting tools set are: two snow cutting knives (Figure 2b) applicable to the bottom of each of the duraluminium tubes with three internal fins designed to prevent the loss of snow at the bottom, dynamometers for the weighting, a shovel for the digging of the trenches, nylon bags with rings to attach the dynamometers to, hammer and wrenches for the screwing of the tubes (Figure 2c). Only in recent years the probes used in some sites were substituted with Teflon probes with similar characteristics.

The measurement procedure of snow depth and density in case of snowpack height lower than 2 m starts with a first check of the snow depth with a graduated rod in order to prepare the instrumentation with the proper number of tubular elements. Then, the instrument is thrust into the snowpack applying a constant pressure and continuous rotational movement until ground level, reading the snow depth measurement on the external notches. Finally, the instrumentation is extracted from the snowpack, depositing the collected sample in a nylon bag to be weighted. In case of snowpack deeper than 2 m, multiple extractions are necessary. A snow pit must be dig up to ground level, paying attention to maintain vertical the front wall. Then, an aluminum plate is inserted horizontally, a first sample is taken from the snowpack surface until the plate is reached and the partial depth measurement is recorded. The procedure is then repeated until the ground level is reached. The bulk



130 snow density is finally computed dividing the weight by the known volume of the sample. In case of snow depth measurement only, a simple graduated rod is adopted.

Each snow depth and bulk snow density measurement is recorded together with the name of the drainage basin, average slope, orientation with respect to the North and elevation. We aggregated data in the six macro-basins described in the previous section in four elevation bands of equal range of 500 m (1000-1500, 1500-2000, 2000-2500 and 2500-3000 m a.s.l.). Overall, 44'411 snow depth and 14'479 bulk snow density measurements were collected and processed. A complete consistency table providing the number of snow depth and bulk snow density measurements for each macro-basin, elevation band and measurement date is reported in the supplementary material.

We performed a preliminary data quality check in order to remove possible erroneous data due to human mistake in the data recording. In case of snow depth, it might happen that a zero is recorded instead of a missing value. Specifically, we checked all the zero snow depth records by comparing them with the closest measurement points. If the snow depth measurements in the locations nearby the equivocal point are larger than a fixed threshold (set at 0.7 m) we consider that zero as a missing value. In the specific case of equivocal measurements in date 15 April, we also checked the previous and following date of measurement of that point. If in that location the snow depth on 1 April and 1 May is larger than 0.7 m we consider the equivocal zero as a missing value. In case of bulk snow density measurements, we removed density values larger than a fixed threshold of 0.75 g cm<sup>-3</sup>, considered far larger than typical bulk snow density values (Allard, 1957; Marbouty, 1980).

145 We used the snow depth and bulk snow density measurements that have passed quality check to estimate the SWE (mm) as

$$SWE = HS \frac{\rho_s}{\rho_w} \quad (1)$$

Where HS (mm) is the snow depth and  $\rho_s$  (kg m<sup>-3</sup>) the bulk snow density and  $\rho_w$  (kg m<sup>-3</sup>) is the liquid water density simply estimated as 1000 kg m<sup>-3</sup>. Since there is not a bulk snow density measurement for each snow depth record, we assigned to  $\rho_s$  the measured snow density only if present. In case of missing bulk snow density value in correspondence to the considered snow depth measurement, we assigned to  $\rho_s$  a mean value computed as the average of the other available snow density values measured in the corresponding date, macro-basin and elevation class. In case there are no density measurements in the corresponding geomorphic class, we consider the SWE data for the specific date, macro-basin and elevation class as missing. Finally, we obtained a timeseries ranging from 1967 to 2020 of average value snow depth and bulk snow density for each macro-basin, elevation class and measurement date.

### 155 2.3 Temperature and precipitation data

Precipitation and temperature are the main meteorological variables regulating accumulation and melting of snow, with air temperature mainly governing the separation of solid and liquid precipitation and driving snowmelt. To evaluate the effects of precipitation and temperature variability on snow depth and SWE in the considered macro-basins, we consider the HISTALP dataset (Auer et al., 2007; Chimani et al., 2011). HISTALP is a multi-century-long (1780-2015) database of monthly homogenized records of temperature, pressure, precipitation, sunshine, and cloudiness for the Alps. Here, we



consider the gridded precipitation and 2 m above ground level air temperature data, provided at 0.08° spatial resolution. Specifically, we considered the average temperature of December, January, February and March over the period 1967-2015. Since 1967, the number of the meteorological stations adopted to create the database and the distance between them have not changed (Auer et al., 2007), making the timeseries sufficiently reliable for the long-term variability and trends analysis. We  
165 extract from the gridded dataset the average temperature over each macro-basin reported in Figure 1. Accordingly, we consider the cumulated precipitation of December, January, February and March. The extracted timeseries are reported in Figure 3.

#### 2.4 North Atlantic Oscillation and Western Mediterranean Oscillation indexes

Following the approach proposed by Ranzi et al. (2021), we evaluate the link of SWE with large scale circulation variability.  
170 Specifically, we consider the North Atlantic Oscillation (NAO) index and the Western Mediterranean Oscillation index (WeMO). NAO is a global circulation pattern index defined as the normalized surface sea-level pressure difference over the North Atlantic Ocean between the Subtropical (Azores) high and Subpolar (Iceland) low. It influences the European climate during winter (Osborn, 2011) and it presents a negative correlation with precipitation in the Italian Alps (Steirou et al., 2017; Zampieri et al., 2017; Brugnara and Maugeri, 2019). WeMO index is a regional teleconnection pattern, spatially limited to  
175 the western Mediterrean basin (Martin-Vide and Lopez-Bustins, 2006). It is defined by the difference of monthly sea-level pressure between the Padua and San Fernando (Cádiz) stations. Here, we consider average DJFM NAO and WeMO indexes to address the links with spring snow depth measured in the considered Alpine basins.

#### 2.5 Statistical and climatological analysis

In order to investigate possible variability and tendencies of snow depth and SWE during the monitored period we adopt  
180 three main methods of statistical analysis. At first, we compute the trend over the complete period 1967 – 2020 by means of a least-square linear regression. To test the statistical significance ( $p$ -value $<0.05$ ) of such trends we adopted the Mann – Kendall (MK) non-parametric test (Mann, 1945; Kendall, 1975) and the parametric Student's  $t$  test on the slope of the regression line, testing the null hypothesis  $H_0$  of no trend against the alternative hypothesis  $H_1$  of linear trend (Rosso and Kottegoda, 2008). Such trend analysis provides only one piece of information, even if important, related to the general  
185 tendency of the studied timeseries. The second analysis consists in a moving average and running trend analysis (MARTA from this point on), similarly to that reported in Brunetti et al. (2009) and Ranzi et al. (2021). MARTA consists in computing running trend and a moving average for all the possible sub-periods longer than 10 years, reporting the results in a chart where the central year of the sub-period is reported on the horizontal axis and its length on the vertical one. In the chart of the running trends, computed by least-square linear regression, slopes are represented by the color of the pixel. We represent  
190 on the plot each trend. However, statistically significant trends according to the MK ( $p$ -value $<0.05$ ) are represented by thicker pixels. In the chart of the moving averages, instead, all the sub-period averages are reported. MARTA is an effective exploratory data analysis and visualization tool, able to capture and highlight periods of values higher or lower than the long



term mean in the timeseries. Here, we extend such approach taken from Brunetti et al. (2009) including a change detection analysis by means of the application of the Pettitt's test (Pettitt, 1979). Pettitt's test is a non-parametric technique to solve the change-point problem (i.e., identifying if and when the probability distribution of a stochastic variable has changed), testing the null hypothesis  $H_0$  of no change. We graphically represent the change-point, if present, in the moving averages chart, indicating the year detected with the statistical test. As third analysis, to evaluate the global behaviour of snow depth and SWE in each basin, we compute the difference between the averages of the two halves of the monitoring period 1967 – 1993 and 1994 – 2020. We test the statistical significance of such differences by means of the non-parametric Mann – Whitney U test (Mann and Whitney, 1947). In this case we test the null hypothesis that the probability of the considered variable between 1967 and 1993 being larger than between 1994 and 2020 is equal to the probability of the considered variable in the latter period being larger than the former.

Finally, we study the relationship and dependencies of snow depth and SWE with variability and changes in climate. We perform the same MARTA analysis to the temperature and precipitation timeseries presented above. Moreover, to evaluate the possible links between snow depth and the teleconnection indexes we evaluated the Pearson's correlation between the snow depth on 1 April and 15 April and the winter (DJFM) NAO and WeMO indexes.

## 2.6 Snow water equivalent model

To compute the SWE it is necessary to have a measurement of both snow depth and bulk snow density (Allard, 1957). Empirical regressions of bulk snow density over day of the year in the Italian Alps have been studied by several authors (e.g., Avanzi et al., 2015; Guyennon et al., 2019). Accordingly, we evaluated the average temporal evolution of bulk snow density during the monitoring period updating with our new dataset the parameters of the model proposed by Guyennon et al. (2019), who found that the temporal evolution of bulk snow density is well described by a quadratic polynomial function of the day of the year as

$$\rho_s(DOY) = n_0 + n_1(DOY + 61) + n_2(DOY + 61)^2 \quad (2)$$

Where  $\rho_s$  is the bulk snow density, DOY is the day of the year.

Snow depth on the ground increases during the accumulation season and start decreasing after the melt onset. Concurrently, positive correlation between snow depth or SWE and elevation in the Alps are reported by many authors (Bavera and De Michele, 2009; Durand et al., 2009; Lehning et al., 2011; Grunewald et al., 2014). Accordingly, we propose a snow depth model linearly dependent on elevation and with time dependent coefficients. For each macro-basin and measurement date we estimate the best fitting linear model of average observed snow depth as a function of elevation as

$$h_s(H, DOY) = m(DOY)[H - H_0(DOY)] \quad (3)$$

Where  $h_s$  is the snow depth, H is the elevation above sea level, m the slope and  $H_0$  the elevation of null snow depth in the regression (snow line elevation). In such way, we reconstruct the elevation dependency of snow depth at different moments of the accumulation and melting seasons. Hence, the temporal dependency is contained in the coefficients m and  $H_0$ ,



225 computed for each available measurement date. In order to obtain a continuous estimate of snow depth as function of both elevation (H) and time (DOY), we fit the computed  $m$  and  $H_0$  using a third-order polynomial curve as

$$m(DOY) = a_0 + a_1DOY + a_2DOY^2 + a_3DOY^3 \quad (4)$$

$$H_0(DOY) = b_0 + b_1DOY + b_2DOY^2 + b_3DOY^3 \quad (5)$$

Where  $a_0$ ,  $a_1$ ,  $a_2$ ,  $a_3$ ,  $b_0$ ,  $b_1$ ,  $b_2$  and  $b_3$  are obtained by a least-square best fitting procedure.

230 By substituting Equation 4 and 5 in Equation 3 and then Equation 2 and 3 in Equation 1, we obtained a simple model to estimate the SWE as function of both elevation and time. The parameters of the proposed model are calibrated for the two periods mentioned above (1967-1993 and 1994-2020) and for each macro-basin. Because of the scarcity of measurements above 2500 m asl, it is not easy to determine whether a maximum threshold is reached at higher altitudes. However, considering that at higher altitudes the major slopes tend to trigger avalanches and the blowing winds tend to prevent snow  
235 deposition, we assume, based also on the available observations, that our altitudinal trends can be extrapolated up to 2500 m asl and a plateau value can be assumed above such altitude. Of course, such threshold is dependent on the topography of the considered basin and a larger number of high-elevation measurements is needed to provide a better estimate of the elevation of the plateau.

### 3 Results and discussion

#### 240 3.1 Snow depth

We computed the temporal trends of snow depth for each macro-basin, elevation class and date of measurement. In Figure 4 we report the timeseries of snow depth for the Toce and Oglio-Chiese-Sarca macro-basins on 1 April and 1 May, together with the equation of the linear model used to estimate the temporal trend. For each case, the snow depth timeseries shows a decreasing trend, with a slightly steeper regression line in case of Oglio-Chiese-Sarca region. The results for each macro-  
245 basin, elevation class and date of measurement are reported in Table 1. The 57% of the cases exhibits a 95% statistically significant decreasing trend according to the MK or Student's  $t$  test, in accordance with the results found by Matiu et al. (2021). We found that absolute value of the long-term trend slopes increases moving from winter (i.e., 1 February and 1 March measurements) to spring (1 and 15 April and 1 May). These are common results across all macro-basins. For the Serio-Brembo macro-basin we obtained the strongest decreasing trend in the elevation class 2000-2500 in the date of 15  
250 April, with a decrease of snow depth of about 0.3 m every decade. The computed trends are coherent with the ones obtained by Schöner et al. (2019) who computed a decrease up to 0.12 m every decade in the southern regions of the Swiss and Austrian Alps for the monitoring period 1961-2012. We report in Figure 5 the MARTA triangles for the same macro-basins of Figure 4. Such graphical representation of the running averages and trends highlights the temporal variability of the timeseries analysed. In the centred moving averages plot is reported the change-point detected by the Pettitt's test. In case of  
255 Toce, we found a change-point in 1985 for the snow depth measured on 1 April while for the Oglio-Chiese-Sarca case we





obtained a statistically significant change-point for both 1 April and 1 May timeseries in 1988 and 1989, respectively. Table 2 contains the statistically significant change-point years detected by the Pettitt's test. The 50% of the cases exhibits a statistically significant change-point according to the Pettitt's test. The change-points obtained range from 1980 to 1992, with 1989 being the mode and 1988 the median. Specifically, the most occurring results are 1986 (frequency  $f=19\%$ ), 1987 (260  $f=19\%$ ), 1988 ( $f=25\%$ ) and 1989 ( $f=26\%$ ). Such late 1980s has first been found by Marty (2007) for the Alpine snow and later confirmed by Reid et al. (2015) at global scale. Finally, we evaluated the difference in average snow depth for each macro-basin, elevation class and date of measurement. Figure 6 shows the average snow depth computed over the monitoring periods 1967-1993 (red circles) and 1994-2020 (black circles). If the difference between the averages of the two samples is statistically significant according to the Mann-Whitney U test, the circles are filled. To improve readability of the plot, an upward or downward blue arrow is reported if an increasing or a decreasing statistically significant trend is present (Table 1), respectively. In case of the Toce basin, at the lower altitudes, a statistically significant difference has been found only in April, together with a statistically significant decreasing trend, with an average decrease of 0.32 m. However, in the elevation class 1500-2000 the difference in snow depth in the two periods is statistically significant from 1 March to 1 June, with a decrease of 0.37 m; in the elevation class 2000-2500 the average difference between the two periods is 0.38 m, statistically significant from 1 April. The Serio-Brembo and Oglio-Chiese-Sarca macro basins exhibits the strongest differences between the two periods, statistically significant for the 90% of the cases. At the two lowest altitudes the difference between the two periods is similar, with an average decrease of 0.28 m (1000-1500) and 0.39 m (1500-2000) for Oglio-Chiese-Sarca and of 0.26 m (1000-1500) and 0.41 m (1500-2000) for Serio-Brembo. In the elevation class 2000-2500 the difference between the two periods in Serio-Brembo macro-basin (0.78 m) is more than twice larger than the one obtained for Oglio-Chiese-Sarca (0.33 m). Measurements of snow depth in the elevation class 2500-3000 show a statistically significant difference of 0.54 m on average starting from 1 April in the Oglio-Chiese-Sarca macro-basin. We found a similar behaviour in Adda basin for the elevation classes 1500-2000 and 2000-2500, with a statistically significant difference of 0.39 m and 0.4 m, respectively. The Adige basin exhibits fewer statistically significant differences, mainly in the two central elevation classes, with an average decrease of 0.21 m (1500-2000) and 0.19 m (2000-2500). In the Piave-Brenta basin the difference in snow depth between the two periods results statistically significant in 89% of the cases at the three lowest elevation classes, with a decrease of 0.21 m (1000-1500) and 0.29 m (1500-2000 and 2000-2500). These results are coherent with the decrease computed by Lejeune et al. (2019) for a mid-altitude (1325 m asl) mountain site in France (Col de Porte). They estimated a decrease of 0.39 m in snow depth between the 1969-1990 and 1991-2017 periods. The results obtained show different trends for the considered regions. In view of this, Matiu et al. (2021) pointed out the difficulties in generalizing the results to the whole Alpine area.

285 Finally, we evaluated the elevation dependency of snow depth in each macro-basin for each measurement date. In Table 3 we report the values of  $m$  and  $H_0$  least-square regression coefficients fitting average snow depth vs altitude in Equation 3. Since the results of the Mann – Whitney U test suggest that there is, in general, a statistically significant difference between the first and second halves of the observation period, we present the results for both 1967 – 1993 and 1994 – 2020 sub-



290 periods. Together with the coefficients obtained from the linear regression analysis, we report the  $R^2$  values for each case as  
an indicator of goodness of the fitting function. The Oglio-Chiese-Sarca, Serio-Brembo and Piave-Brenta macro-basins show  
higher values of  $R^2$  and a common behaviour of  $m$  and  $H_0$ . In fact, in these basins,  $m$  increases after February (accumulation)  
showing a peak value in spring, reinforced by the earlier onset of the melting season at lower elevations, and then decreases  
as melting develops at higher elevations. In fact, during the accumulation period the principal factor affecting  $m$  is the  
295 change from rain to snow with elevation while during the melt period it is more affected by the variation in melt with  
elevation (Allard, 1957). On the other hand,  $H_0$  exhibits an almost stable or decreasing behaviour during the accumulation  
phase, strongly increasing as the melting season starts. We also observe that  $H_0$  exhibits higher values in the second half of  
the monitoring period, indicating that the elevation of null snow depth has moved towards higher altitudes, accordingly to  
the hypothesis of decreasing snow depth. Such results confirm the tendency modelled by Giorgi et al. (1997) who studied the  
300 elevation dependency of surface climate change impacting snow depth over the Alpine region. The results obtained for  
Adige, Adda and Toce basins show less reliable results according to the lower values of  $R^2$  obtained and the physically  
meaningless negative values of  $H_0$ , mainly due to the lower number of snow depth measurements.

### 3.2 Snow density

In order to investigate possible variability and tendencies of snow depth and SWE, we evaluated bulk snow density data  
305 variations with elevation and in time. In Figure 7 we show the bulk snow density plotted as a function of the elevation, for  
the six considered measurement dates, in the Piave-Brenta macro basin. We found that, within each elevation class, bulk  
snow density does not substantially vary with elevation for a specific measurement date. On the other hand, we found that  
bulk snow density increases with measuring date. Such behaviour is common among all the macro-basins studied. In Figure  
8 we report the average bulk snow density computed over the monitoring period. From a least-square fitting of Equation 2  
310 we obtained new values for the polynomial coefficients, better modelling the data here presented ( $R^2=0.998$ ) and compared  
with the model from Guyennon et al. (2019). Specifically, we obtained  $n_0=277$ ,  $n_1*10^{-1}=-3.6$  and  $n_2*10^{-3}=5.1$ . Such seasonal  
increase of snow density is related to different processes such as compaction, increase of liquid water in the snowpack due to  
melting as the temperature increases.

### 3.3 Snow water equivalent

315 For the available SWE estimates, we computed the temporal trends for each macro-basin, elevation class and date of  
measurement. In Table 4 we report the temporal trends computed over the monitoring period 1967-2020. Obviously, the  
general behaviour is in accordance with the one found in case of snow depth, showing a decreasing trend. Among the  
considered timeseries, we obtained statistically significant trends in 44% of the cases according to the MK or Student's  $t$  test,  
mainly in the Oglio-Chiese-Sarca macro-basin. In this macro-basin, the computed trends increase in terms of absolute value  
320 moving from winter to spring in the two lower elevation classes, reaching the maximum between 15 April (-36 mm every  
decade for 1000-1500) and 1 May (-67 mm every decade for 1500-2000); in the two higher elevation classes we found



statistically significant trends for the measurement dates of 15 April, 1 May and 1 June, suggesting that the spring snow has been more strongly affected in the past decades, reaching the maximum absolute value in May (-48 mm every decade for 2000-2500 and -67 mm every decade for 2500-3000). In Table 5 we report the results of the change-point analysis performed  
325 by means of the Pettitt's test. The change-points obtained range from 1986 to 1991, with 1988 being both mode and median. Specifically, the most occurring change-point years are 1989 ( $f=17\%$ ), 1986 ( $f=27\%$ ) and 1988 ( $f=46\%$ ). The Pettitt's test confirms on a sound statistical basis the findings of other studies, such as Marty et al. (2017), based on SWE measurements, and Colombo et al. (2022), based on snow depth measurements and SWE modelling. Valt and Cianfarra (2009) obtained similar results, finding breakpoints between 1984 and 1994. Also in this case, the Oglio-Chiese-Sarca macro-basin exhibits  
330 statistically significant results for the largest cases of elevation classes and measurement dates. For this specific macro-basin, we found the statistically significant change points mainly April and May, in agreement with the results obtained for the long-term trends. As for the case of snow depth, we evaluated the difference in average SWE for each macro-basin, elevation class and date of measurement. In Figure 9 we report the average SWE computed over the monitoring periods 1967-1993 (red circles) and 1994-2020 (black circles). The Oglio-Chiese-Sarca macro-basins presents statistically significant results in  
335 most cases. We found that the largest statistically significant differences in SWE between the two periods is in Spring, for the measurement dates of 1 April and 15 April for the 1000-1500 elevation class and 15 April and 1 May for the other cases. The average difference between the two periods is 85 mm for the elevation class 1000-1500, 135 mm for 1500-2000, 104 mm for 2000-2500 and 226 mm for 2500-3000. The Piave-Brenta macro-basin shows similar results, with statistically significant differences in 89% of the cases. We found the largest statistically significant differences on 1 April and 15 April  
340 for the 1000-1500 elevation class, with an average difference of 59 mm, on 15 April and 1 May for the 1500-2000 elevation class, with an average difference of 82 mm, and 1 May and 1 June for 2000-2500 elevation class, with an average difference of 78 mm. For the Adige basin we found statistically significant differences mainly in the 1500-2000 elevation class, with an average difference of 70 mm. For the Toce and Serio-Brembo macro-basins the estimate of SWE appears less robust than in the other basins, mainly because of the fewer available measurements of bulk snow density, resulting in more scattered  
345 timeseries in Figure 9. The Adda basin exhibits statistically significant differences in the 1500-2000 and 2000-2500 elevation classes, with an average difference of 141 mm and 104 mm, respectively. Similarly, Marty et al. (2017) observed a stronger decrease of SWE at higher altitudes. Moreover, they also found larger decreases for April SWE than for February SWE, in agreement with our results.

### 3.4 Climate variability

350 In order to evaluate possible links between climate variability and changes occurred during the monitoring period and the amount and persistence of snow in the considered macro-basins, we performed the MARTA analysis to temperature and precipitation data. Specifically, we considered the average DJFM precipitation and temperature obtained from the HISTALP dataset. We report the results of the precipitation analysis in Figure 10 and the temperature analysis in Figure 11. For all the considered macro-basins, DJFM precipitation exhibits a slight non-significant decrease over the monitoring period and no



355 statistically significant change-point is detected according to the Pettitt's test (Figure 10). By looking at the sub-periods  
between 10 and 20 years, it is possible to notice three areas of statistically significant trends, showing an increase before  
1980, a decrease around 1990 and another increase around 2000, confirming a non-uniform tendency over the complete  
monitoring period. We also performed the same statistical analysis to the HISTALP mean monthly temperature averaged  
over all the basins (not shown here), to evaluate possible differences in climate variability between accumulation and melting  
360 seasons. Temperature increases significantly in both the accumulation (from January to March) and, even more significantly,  
the melting period (April and May), consistently with results reported by many authors as Auer et al. (2007) and Brunetti et  
al. (2009). These results explain the decrease in snow depth and SWE on 1 April and the accelerated melt on 15 April – 1  
June period. Both winter (DJFM) and spring (April and May) temperatures exhibit a marked increase after 1987, where a  
change-point is detected by the Pettitt's test. This result is consistent with the change-point detected in the snow depth and  
365 SWE timeseries, suggesting a strong impact of temperature increase, especially in spring, on snowmelt. The combined effect  
of precipitation and temperature variability is consistent with the observed stationarity of winter (February and March) snow  
depth and SWE, the significant decrease of the maximum SWE observed in April and the accelerated melt in May. Marty et  
al. (2017) found similar result, linking the strong low elevation SWE decreases to temperature increases and decreasing  
snow/rain ratio. These results confirm the impact of temperature rise on snow, affecting consequently the hydrological cycle  
370 and water availability.

Finally, we evaluated the correlation between snow depth on 1 and 15 April and the DJFM NAO and WeMO indexes. In  
Figure 12 we report the matrixes of statistically significant Pearson's correlations, where the rows represent the six macro-  
basins and the columns the four elevation classes. We obtain a negative statistically significant Pearson's correlation  
between winter NAO and spring snow depth ranging between -0.30 and -0.55 for 1 April and between -0.29 and -0.49 for 15  
375 April. These results are coherent with previous studies of several authors as Steirou et al. (2017) who found linkages  
between NAO and precipitation in Europe; Colombo et al. (2022) found a negative correlation between NAO and SWE  
indexes. The WeMO index exhibits an opposite link with snow depth, with positive statistically significant correlation  
ranging between 0.27 and 0.37 for 1 April and between 0.27 and 0.40 for 15 April, in agreement with the positive correlation  
between winter WeMO and precipitation (0.38) obtained by Ranzi et al. (2021).

### 380 **3.5 SWE model**

Here we show the results obtained from the SWE regression model presented in Section 2.6, applied to the case of Oglio-  
Chiese-Sarca macro-basin. In Figure 13 we show the values of  $m$  (a) and  $H_0$  (b) obtained from the linear regression analysis  
of average snow depth measurements for the monitoring period 1994-2020 (black diamonds) obtained from Table 3. We  
selected the Oglio-Chiese-Sarca macro basin as it shows the highest  $R^2$  values (Table 3) and the second half of the  
385 monitoring period as more representative of the current nivological situation. The best fitting of Equation 4 and 5 are plotted  
as dotted black lines and the coefficients  $a_0$ ,  $a_1$ ,  $a_2$ ,  $a_3$ ,  $b_0$ ,  $b_1$ ,  $b_2$  and  $b_3$  are reported as well, together with  $R^2$  values. The  
fitting curves well describe the observed behaviour presented in Section 2.1, showing high values of  $R^2$  (0.97 for  $m$  and 0.99



for  $H_0$ ). Such fitting must be considered valid only within the considered time period, as it might introduce strong uncertainty due to the low number of points adopted for the fitting procedure. However, the curve obtained provides an analytical function to estimate the temporal evolution of the linear regression coefficients  $m$  and  $H_0$ . Hence, the following equation can be written to model the SWE as function of time and elevation.

$$SWE(H, DOY) = m(DOY)[H - H_0(DOY)] \frac{\rho_s(DOY)}{\rho_w} \quad (6)$$

The coefficients  $n_0$ ,  $n_1$ ,  $n_2$ , to define the second-order polynomial function of  $\rho_s$  are reported in Section 3.2. With the estimates of  $m$ ,  $H_0$  and  $\rho_s$  obtained from the long-term snow depth and bulk snow density observations it is possible to estimate the SWE in the DOY-H space as shown in Figure 14. From the contour plot, we observe that the DOY of maximum SWE for fixed elevation (DOY of the local minimum of the SWE isolines) linearly shifts in time, confirming the behaviour observed in the previous sections. However, for elevations higher than 2500 m asl, we consider the model less reliable as the number of snow depth measurements is lower at such elevation and above a certain point snow depth might reach a plateau or even decrease (Grünewald et al., 2014). This model must be intended in a climatological way, as it has been conceived from average values over a time period of 27 years, and it can provide a simple yet useful estimate of the expected snow water equivalent at a given day of the year and

#### 4 Conclusions

We studied changes and variability of snow depth and SWE in six macro-basins of the Italian Alps over the monitoring period 1967-2020 based on measurements collected on 1 February, 1 March, 1 April, 15 April, 1 May and 1 June. Our results show the effects of the temperature increase of the past century on snow accumulation in the Italian Alps. We found statistically significant decreasing trends in both snow depth ( $-0.12$  m decade<sup>-1</sup> on average in the Oglio-Chiese-Sarca basin) and SWE ( $-37$  mm decade<sup>-1</sup> on average in the Oglio-Chiese-Sarca basin) over the years and a statistically significant decrease of snow depth and SWE between the two halves of the monitoring period (1967-1993 and 1994-2020). Specifically, we found that, on average, snow depth decreased of 33% on 1 April, exhibiting stronger differences between the two periods at lower altitudes (62% in the 1000-1500 m elevation class) and smaller difference towards higher elevations (30% at 1500-2000 m, 22% at 2000-2500 m and 18% at 2500-3000 m). In case of SWE we found an decrease of 32% with respect to the 1967-1993 period, higher at low elevations (52% at 1000-1500 m) and substantially lower at higher altitudes (between 28% and 29%). These overall mean results are computed as the average of all the observed percentage decrease on 1 April including all considered basins, with the first value accounting for all the elevations and the following ones specific for elevation class. Such results have been also confirmed by the higher values of snow line elevation  $H_0$  we obtained. The computed trends and differences exhibit a strong change in spring (1 April and 15 April mainly) snow depth and SWE, suggesting that spring snowmelt is highly impacted by global warming. Such behaviour can have strong effects on the



hydrological regime of the considered catchments, possibly modifying magnitude and timing of flood events and affecting water availability in the summer.

420 We found that around 1988, on average, there has been a change-point, with snow depth and SWE being lower in the following decades. This appears to be a common result for all the macro-basins and elevations. To reject the hypothesis of possible errors in the snow depth and SWE timeseries due to measurement methodology variations or other factors affecting the timeseries reliability, we performed the same change-point detection analysis on measured temperature data from HISTALP dataset, resulting in a change-point in the same period. This result confirms the robustness of our findings and  
425 highlights the strong effects of temperature on snow amount and persistency, both in terms of rain-snow separation and melt onset. The analysis of precipitation and temperature data also confirms the weaker variation during the accumulation season (1 February and 1 March) in contrast with the strong decrease in snow depth and SWE during the melting season. The correlation analysis of NAO and WeMO climatological indexes with snow depth on 1 April showed similar correlations obtained in other studies. In fact, we found negative Pearson's correlation coefficient in case of NAO index and positive in  
430 case of WeMO index. Further investigations might highlight the impacts of the observed changes in climatological and nivological conditions on hydropower energy production.

The elevation and time dependency analysis of snow depth and bulk snow density measurements allowed us developing a simple SWE model as a function of time and elevation. In fact, as shown in Figure 8, bulk snow density changes significantly only with the day of the year, being almost constant with altitude. On the other hand, snow depth linearly  
435 increases with elevation and, of course, increases along the accumulation season and start decreasing as the melting season begins. From such analysis we obtained the parameters for a simple SWE model that can be applied to estimate the SWE evolution between February and July as function of the elevation and day of the year. Such model can be used to estimate SWE for local applications in the considered macro basins.

### Data availability

440 The dataset of snow depth and bulk snow density used for this study was provided by ENEL and it will be made available upon request. The HISTALP dataset is available at <https://www.zamg.ac.at/histalp/datasets.php> (last access, 04/07/2023). The climate oscillation indexes are available at <https://www.ncei.noaa.gov/access/monitoring/products/> (NAO, last access 04/07/2023) and at <http://www.ub.edu/gc/wemo/> (WeMO, last access 04/07/2023).

### Contributions

445 RR, PC and GG designed the study and the methodology. PC processed the data and prepared the figures. RR and PC wrote the text. RR, PC and GG edited and reviewed the manuscript.



## Competing interests

The authors declare that they have no conflict of interest.

## Acknowledgments

450 Fundings for this study has been provided by Cariplo Foundation through the CLIMADA project and by Po River basin  
Authority through the grant number 8536/2020. We gratefully thank the Hydrology and Hydraulic Analysis center of Enel  
Green Power in Venice-Mestre for the data made available and the collaboration over the last decades. The preliminary  
results of this research have been presented at AGU Fall Meeting 2021 (Colosio et al., 2021). We would like to thank Paolo  
Raccagni and Vladimiro Boselli for their contribution at the earliest stage of the project and Mauro Valt (ARPA Veneto) for  
455 his comments.

## References

- Allard, W.: Snow Hydrology: Summary Report of the Snow Investigations. Published by the North Pacific Division, Corps  
of Engineers, US Army, Portland, Oregon, 1956.
- Auer, I., Böhm, R., Jurkovic, A., Lipa, W., Orlik, A., Potzmann, R., Schöner, W., Ungersbock, M., Matulla, C., Briffa, K.,  
460 Jones, P., Efthymiadis, D., Brunetti, M., Nanni, T., Maugeri, M., Mercalli, L., Mestre, O., Moisselin, J.-M., Begert, M.,  
Muller- Westermeier, G., Kveton, V., Bochnicek, O., Stastny, P., Lapin, M., Szalai, S., Szentimrey, T., Cegnar, T., Dolinar,  
M., GajicCapka, M., Zaninovic, K., Majstorovic, Z. and Nieplova, E.: HISTALP—historical instrumental climatological  
surface time series of the Greater Alpine Region, *International Journal of Climatology: A Journal of the Royal  
Meteorological Society*, 27(1), 17-46, 2007.
- 465 Avanzi, F., De Michele, C., and Ghezzi, A.: On the performances of empirical regressions for the estimation of bulk snow  
density, *Geografia Fisica e Dinamica Quaternaria*, 38(2), 105-112, 2015.
- Bavera, D., and De Michele, C.: Snow water equivalent estimation in the Mallerio basin using snow gauge data and MODIS  
images and fieldwork validation, *Hydrological Processes: An International Journal*, 23(14), 1961-1972, 2009.
- Beniston, M.: Is snow in the Alps receding or disappearing?, *Wiley Interdisciplinary Reviews: Climate Change*, 3(4), 349-  
470 358, 2012.
- Beniston, M., Farinotti, D., Stoffel, M., Andreassen, L. M., Coppola, E., Eckert, N., Fantini, A., Giacomoni, F., Hauck, C.,  
Huss, M., Huwald, H., Lehning, M., López-Moreno, J.-I., Magnusson, J., Marty, C., Morán-Tejeda, E., Morin, S., Naaim,  
M., Provenzale, A., Rabatel, A., Six, D., Stötter, J., Strasser, U., Terzago, S. and Vincent, C.: The European mountain  
cryosphere: a review of its current state, trends, and future challenges, *The Cryosphere*, 12(2), 759-794, 2018.
- 475 Blöschl, G.: Scaling issues in snow hydrology, *Hydrological processes*, 13(14-15), 2149-2175, 1999.



- Bocchiola, D., and Diolaiuti, G.: Evidence of climate change within the Adamello glacier of Italy, *Theoretical and Applied Climatology*, 100 (3), 351–369, 2009.
- Bugnara, Y., and Maugeri, M.: Daily precipitation variability in the southern Alps since the late 19th century, *International journal of climatology*, 39(8), 3492-3504, 2019.
- 480 Brunetti, M., Lentini, G., Maugeri, M., Nanni, T., Auer, I., Boehm, R., and Schöener, W.: Climate variability and change in the greater alpine region over the last two centuries based on multi-variable analysis, *International Journal of Climatology*, 29 (15), 2197–2225, 2009.
- Chimani, B., Böhm, R., Matulla, C., and Ganekind, M.: Development of a longterm dataset of solid/liquid precipitation, *Advances in Science and Research*, 6(1), 39-43, 2011.
- 485 Colombo, N., Valt, M., Romano, E., Salerno, F., Godone, D., Cianfarra, P., Freppaz, M., Maugeri, M., and Guyennon, N.: Long-term trend of snow water equivalent in the Italian Alps, *Journal of Hydrology*, 614, 128532, 2022.
- Colosio, P., Ranzi, R., Boselli, V., Raccagni, P., and Galeati, G.: Climatology of snow depth and snow water equivalent in the Italian Alps (1967-2020), in *AGU Fall Meeting Abstracts (Vol. 2021, pp. C35G-0953)*, 2021.
- Durand, Y., Giraud, G., Laternser, M., Etchevers, P., Mérindol, L., and Lesaffre, B.: Reanalysis of 47 years of climate in the  
490 French Alps (1958–2005): climatology and trends for snow cover, *Journal of applied meteorology and climatology*, 48(12), 2487-2512, 2009.
- Fontrodona Bach, A., Van der Schrier, G., Melsen, L. A., Klein Tank, A. M. G., and Teuling, A. J.: Widespread and accelerated decrease of observed mean and extreme snow depth over Europe, *Geophysical Research Letters*, 45(22), 12-312, 2018.
- 495 Ge, Y., and Gong, G.: North American snow depth and climate teleconnection patterns, *Journal of Climate*, 22(2), 217-233, 2009.
- Giorgi, F., Hurrell, J. W., Marinucci, M. R., and Beniston, M.: Elevation dependency of the surface climate change signal: a model study, *Journal of Climate*, 10(2), 288-296, 1997.
- Grünewald, T., Bühler, Y., and Lehning, M.: Elevation dependency of mountain snow depth, *The Cryosphere*, 8(6), 2381-  
500 2394, 2014.
- Guyennon, N., Valt, M., Salerno, F., Petrangeli, A. B., and Romano, E.: Estimating the snow water equivalent from snow depth measurements in the Italian Alps, *Cold Regions Science and Technology*, 167, 102859, 2019.
- Kendall, M.: *Rank Correlation Methods*, 4th edition, London, Charles Griffin, 1975.
- Lehning, M., Grünewald, T., and Schirmer, M.: Mountain snow distribution governed by an altitudinal gradient and terrain  
505 roughness, *Geophysical Research Letters*, 38(19), 2011.
- Lehr, C., Ward, P. J., and Kummu, M.: Impact of large-scale climatic oscillations on snowfall-related climate parameters in the world's major downhill ski areas: a review, *Mountain Research and Development*, 32(4), 431-445, 2012.





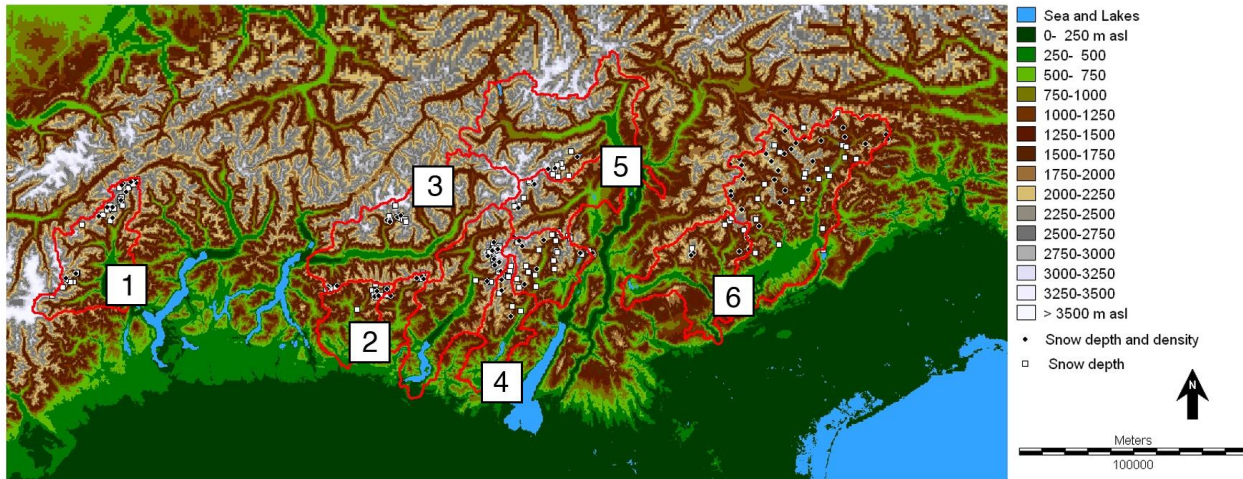
- Lejeune, Y., Dumont, M., Panel, J. M., Lafaysse, M., Lapalus, P., Le Gac, E., Lesaffre, B., and Morin, S.: 57 years (1960–2017) of snow and meteorological observations from a mid-altitude mountain site (Col de Porte, France, 1325 m of altitude), *Earth System Science Data*, 11(1), 71–88, 2019.
- López-Moreno, J. I., Soubeyroux, J. M., Gascoïn, S., Alonso-Gonzalez, E., Durán-Gómez, N., Lafaysse, M., Vernay, M., Carmagnola, C., and Morin, S.: Long-term trends (1958–2017) in snow cover duration and depth in the Pyrenees, *International Journal of Climatology*, 40(14), 6122–6136, 2020.
- Mann, H.B.: Nonparametric tests against trend, *Econometrica: Journal of the Econometric Society*, 13, 245–259, 1945.
- 515 Mann, H. B., and Whitney, D. R.: On a test of whether one of two random variables is stochastically larger than the other, *The annals of mathematical statistics*, 50–60, 1947.
- Marbouty, D.: An experimental study of temperature-gradient metamorphism, *Journal of Glaciology*, 26(94), 303–312, 1980.
- Marcolini, G., Bellin, A., Disse, M., and Chiogna, G.: Variability in snow depth time series in the Adige catchment. *Journal of Hydrology: Regional Studies*, 13, 240–254, 2017.
- 520 Martin-Vide, J., and Lopez-Bustins, J. A.: The western Mediterranean oscillation and rainfall in the Iberian Peninsula, *International Journal of Climatology: A Journal of the Royal Meteorological Society*, 26(11), 1455–1475, 2006.
- Marty, C., Tilg, A. M., and Jonas, T.: Recent evidence of large-scale receding snow water equivalents in the European Alps. *Journal of Hydrometeorology*, 18(4), 1021–1031, 2017.
- Matiu, M., Crespi, A., Bertoldi, G., Carmagnola, C. M., Marty, C., Morin, S., Schöner, W., Cat Berro, D., Chiogna, G., De  
525 Gregorio, L., Kotlarski, S., Majone, B., Resch, G., Terzago, S., Valt, M., Beozzo, W., Cianfarra, P., Gouttevin, I., Marcolini, G., Natarnicola, C., Petitta M., Scherrer, S. C., Strasser, U., Winkler, M., Zebisch, M., Cicogna, A., Cremonini, R., Debernardi, A., Faletto, M., Gaddo, M., Giovannini, L., Mercalli, L., Soubeyroux, J. M., Sušnik, A., Trenti, A., Urbani, S., and Weilguni, V.: Observed snow depth trends in the European Alps: 1971 to 2019, *The Cryosphere*, 15(3), 1343–1382, 2021.
- 530 Osborn, T.: Winter 2009/2010 temperatures and a record-breaking North Atlantic Oscillation index, *Weather*, 66(1), 19–21, 2011.
- Penna, D., van Meerveld, H. J., Zuecco, G., Dalla Fontana, G., and Borga, M.: Hydrological response of an Alpine catchment to rainfall and snowmelt events, *Journal of Hydrology*, 537, 382–397, 2016.
- Pettitt, A. N.: A non-parametric approach to the change-point problem, *Journal of the Royal Statistical Society: Series C (Applied Statistics)*, 28(2), 126–135, 1979.
- 535 Portner, H.O., Roberts, D.C., Masson-Delmotte, V., Zhai, P., Tignor, M., Poloczanska, E., Mintenbeck, K., Nicolai, M., Okem, A., Petzold, J. and Rama, B.: IPCC, 2019: IPCC Special Report on the Ocean and Cryosphere in a Changing Climate, 2019.
- Pulliainen, J., Luojus, K., Derksen, C., Mudryk, L., Lemmetyinen, J., Salminen, M., Ikonen, J., Takala, M., Cohen, J.,  
540 Smolander, T., and Norberg, J.: Patterns and trends of Northern Hemisphere snow mass from 1980 to 2018, *Nature*, 581(7808), 294–298, 2020.



- Ranzi, R., Grossi, G., and Bacchi, B.: Ten years of monitoring areal snowpack in the southern alps using noaa-avhrr imagery, ground measurements and hydrological data, *Hydrological Processes*, 13 (12-13), 2079–2095, 1999.
- Ranzi, R., Grossi, G., Gitti, A., and Taschner, S.: Energy and mass balance of the Mandrone glacier (Adamello, central alps),  
545 *Geografia Fisica e Dinamica Quaternaria*, 33 (1), 45–60, 2010.
- Ranzi, R., Michailidi, E. M., Tomirotti, M., Crespi, A., Brunetti, M., and Maugeri, M.: A multi-century meteo-hydrological analysis for the Adda river basin (Central Alps). Part II: Daily runoff (1845–2016) at different scales, *International Journal of Climatology*, 41(1), 181-199, 2021.
- Reynard, E.: Mountain Tourism and Water and Snow Management in Climate Change Context, *Journal of Alpine Research* |  
550 *Revue de géographie alpine*, (108-1), 2020.
- Rignot, E., Velicogna, I., van den Broeke, M. R., Monaghan, A. and Lenaerts, J. T. M.: Acceleration of the contribution of the Greenland and Antarctic ice sheets to sea level rise, *Geophys. Res. Lett.*, 38(5), 2011.
- Schaefli, B., Hingray, B., and Musy, A.: Climate change and hydropower production in the Swiss Alps: quantification of potential impacts and related modelling uncertainties, *Hydrology and Earth System Sciences*, 11(3), 1191-1205, 2007.
- 555 Schöner, W., Koch, R., Matulla, C., Marty, C., and Tilg, A. M.: Spatiotemporal patterns of snow depth within the Swiss-Austrian Alps for the past half century (1961 to 2012) and linkages to climate change, *International Journal of Climatology*, 39(3), 1589-1603, 2019.
- Serreze, M. C., Clark, M. P., Armstrong, R. L., McGinnis, D. A., and Pulwarty, R. S.: Characteristics of the western United States snowpack from snowpack telemetry (SNOTEL) data, *Water Resources Research*, 35(7), 2145-2160, 1999.
- 560 Steirou, E., Gerlitz, L., Apel, H., and Merz, B.: Links between large-scale circulation patterns and streamflow in Central Europe: A review, *Journal of hydrology*, 549, 484-500, 2017.
- Tapley, B. D., Bettadpur, S., Watkins, M., and Reigber, C.: The gravity recovery and climate experiment: Mission overview and early results, *Geophysical research letters*, 31(9), 2004.
- Taschner, S., Ranzi, R., Bacchi, B., and Galeati, G.: Monitoring the snow water equivalent in the Piave headwater applying a  
565 remotely sensed based approach, in *IGARSS 2004, 2004 IEEE International Geoscience and Remote Sensing Symposium (Vol. 6, pp. 3692-3695)*, 2004.
- Takala, M., Luojus, K., Pulliainen, J., Derksen, C., Lemmetyinen, J., Kärnä, J. P., Koskinen, J., and Bojkov, B.: Estimating northern hemisphere snow water equivalent for climate research through assimilation of space-borne radiometer data and ground-based measurements. *Remote Sensing of Environment*, 115(12), 3517-3529, 2011.
- 570 Tedesco, M., Derksen, C., Deems, J. S., and Foster, J. L.: Remote sensing of snow depth and snow water equivalent. *Remote Sensing of the Cryosphere*, 73-98, 2015.
- Terzago, S., Cassardo, C., Cremonini, R., and Fratianni, S.: Snow precipitation and snow cover climatic variability for the period 1971–2009 in the southwestern Italian Alps: The 2008–2009 snow season case study, *Water*, 2(4), 773-787, 2010.
- Valt, M., and Cianfarra, P.: Recent snow cover variability in the Italian Alps. *Cold Regions Science and Technology*, 64(2),  
575 146-157, 2010.

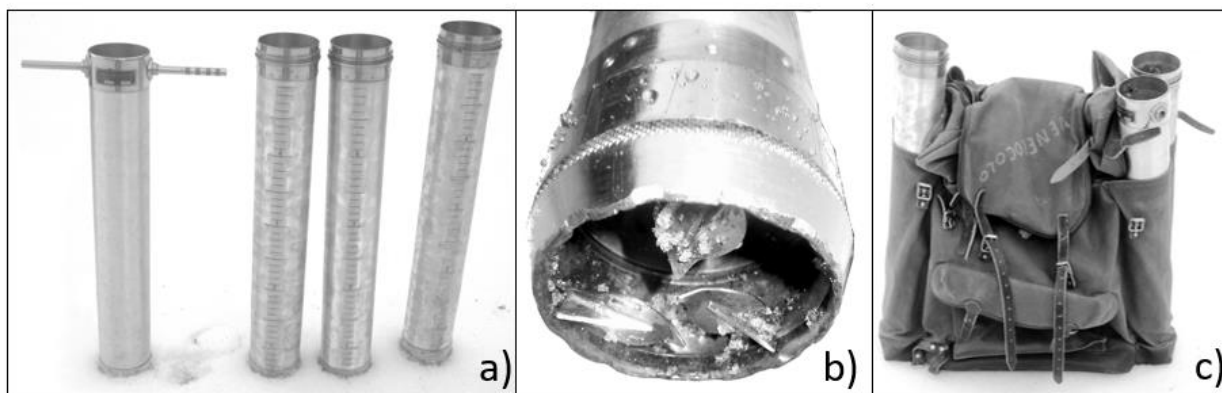


Zampieri, M., Toreti, A., Schindler, A., Scoccimarro, E., and Gualdi, S.: Atlantic multi-decadal oscillation influence on weather regimes over Europe and the Mediterranean in spring and summer, *Global and Planetary Change*, 151, 92-100, 2017.



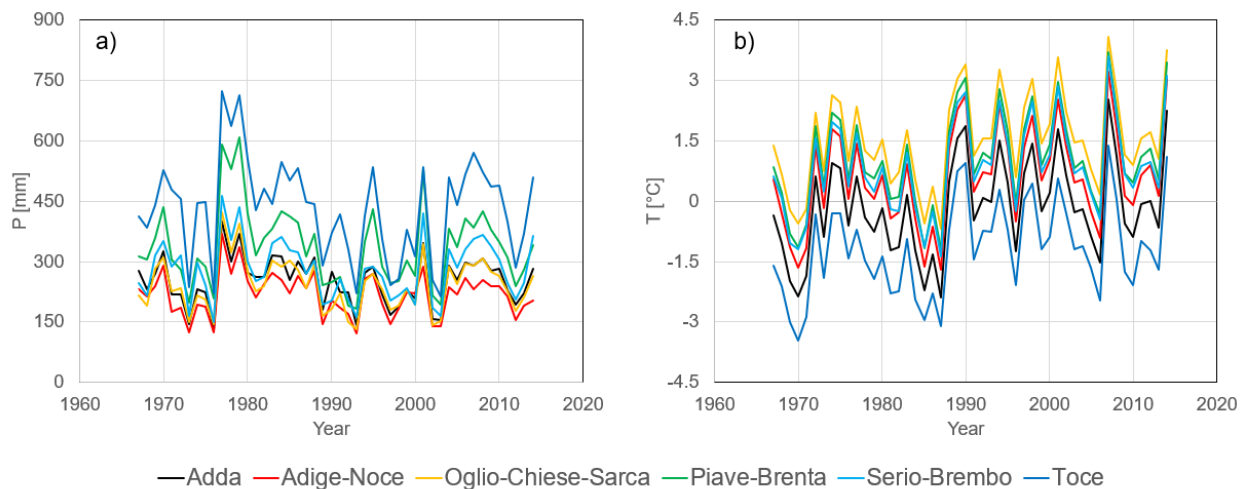
580

**Figure 1: Map of the research area. The individual basins are grouped in the six macro basins by number: (1) Toce, (2) Serio-Brembo, (3) Adda, (4) Oglio-Chiese-Sarca, (5) Adige and (6) Piave-Brenta. Locations of snow depth and density (black dots) and snow depth (white squares) are also reported.**

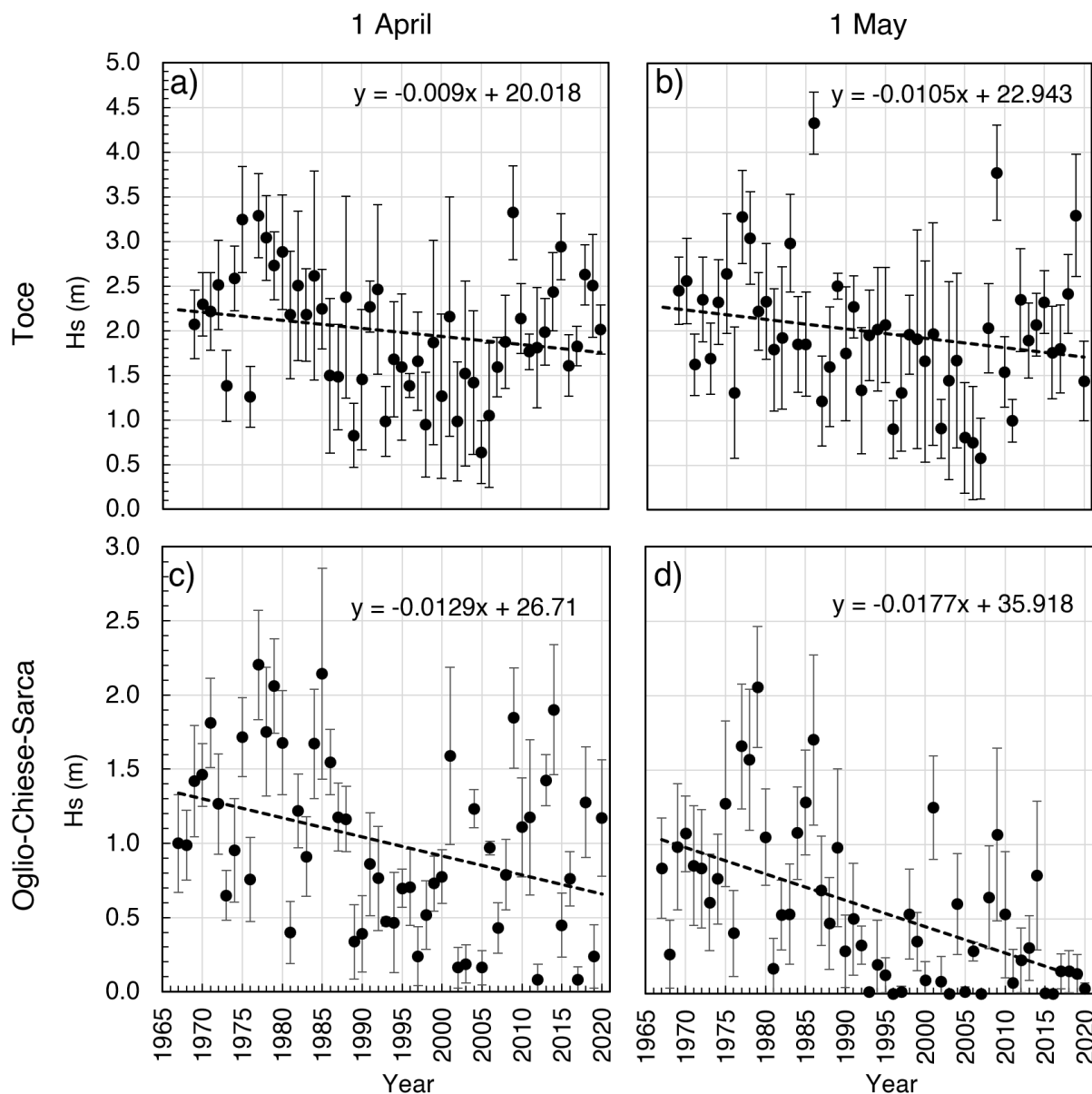


585

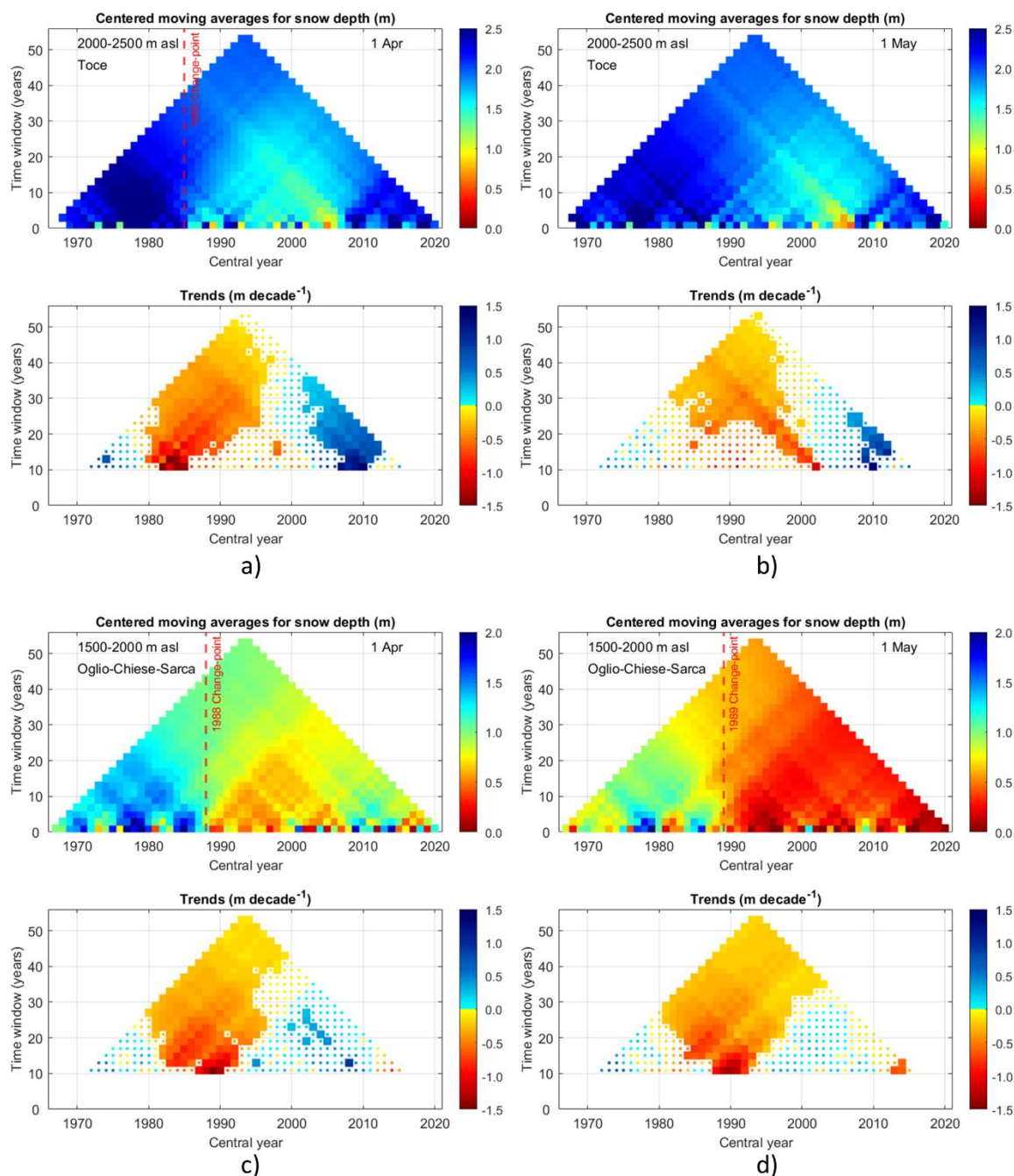
**Figure 2: Photo of (a) CN2 type snow sampler and (b) detail of the cutting knife with the three internal fins and (c) the complete kit in its transporting bag.**



590 **Figure 3: Timeseries of (a) cumulated precipitation and (b) air temperature averaged over the period DJFM from the HISTALP dataset, spatially averaged over the six macro-basins areas.**

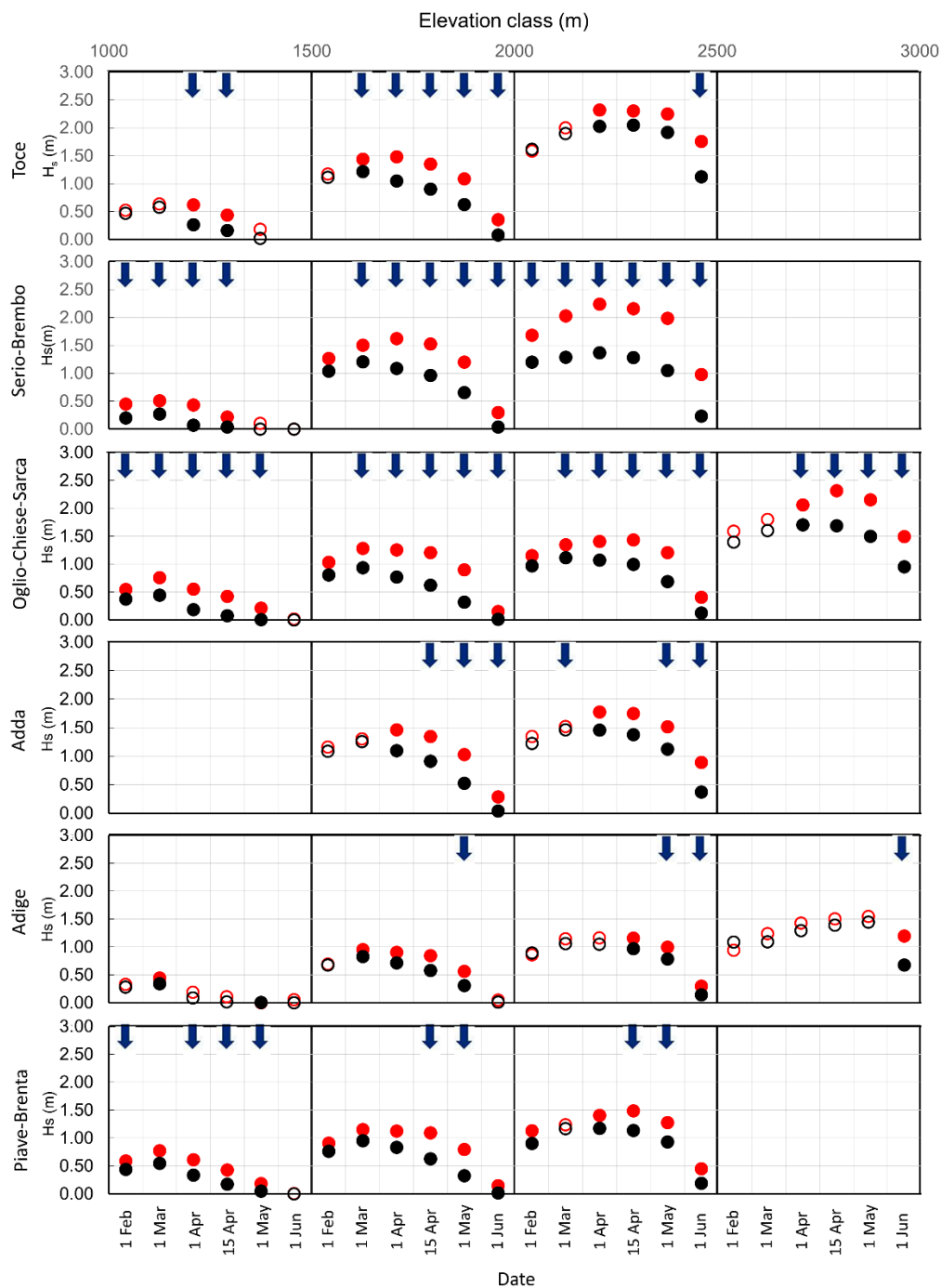


595 **Figure 4: Time series average of snow depth (black dots) in Toce (a, b) and Oglio-Chiese-Sarca (c, d) macro-basins on 1 April (a, c) and 1 May (b, d). Error bars indicate the standard deviation over the specific macro-basin and dashed lines the least-square interpolation line.**

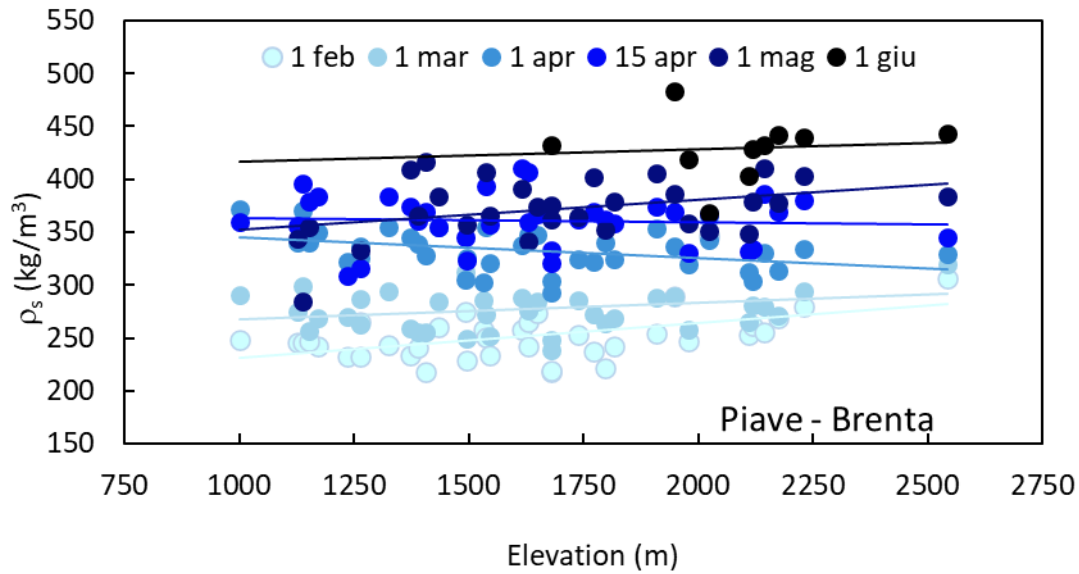


600 **Figure 5: Moving Average and Running Trend Analysis (MARTA triangles) of snow depth on 1 April (a, c) and 1 May (b, d) in the altitudinal class 1500-2000 m asl for the Toce and 2000-2500 m asl for the Oglio – Chiese – Sarca macro-basins. In the top part of each panel the statistically significant change point detected by the Pettitt’s test (5% significance) is reported as dashed line while in the bottom part the statistically significant trends with 5% significance level of the Mann-Kendall test are reported as thicker pixels.**



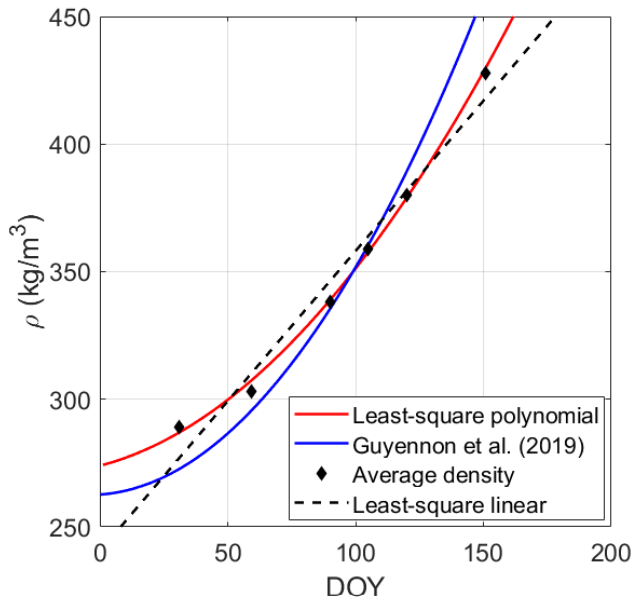


605 **Figure 6:** Average snow depth (Hs) in the 1967-1993 (red circles) and in 1994-2020 (black circles) periods are plotted for each elevation class in the six observation campaigns dates (1 Feb, 1 Mar, 1 Apr, 15 Apr, 1 May, 1 Jun). Statistically significant ( $p \leq 0.01$ , Mann-Kendall test) trends of the entire 1967-2020 period are sketched as upward (downward) blue arrow for increasing (decreasing) trends. Circles are filled if the difference of Hs between the two periods is statistically significant ( $p \leq 0.01$ , Mann-Whitney U test).

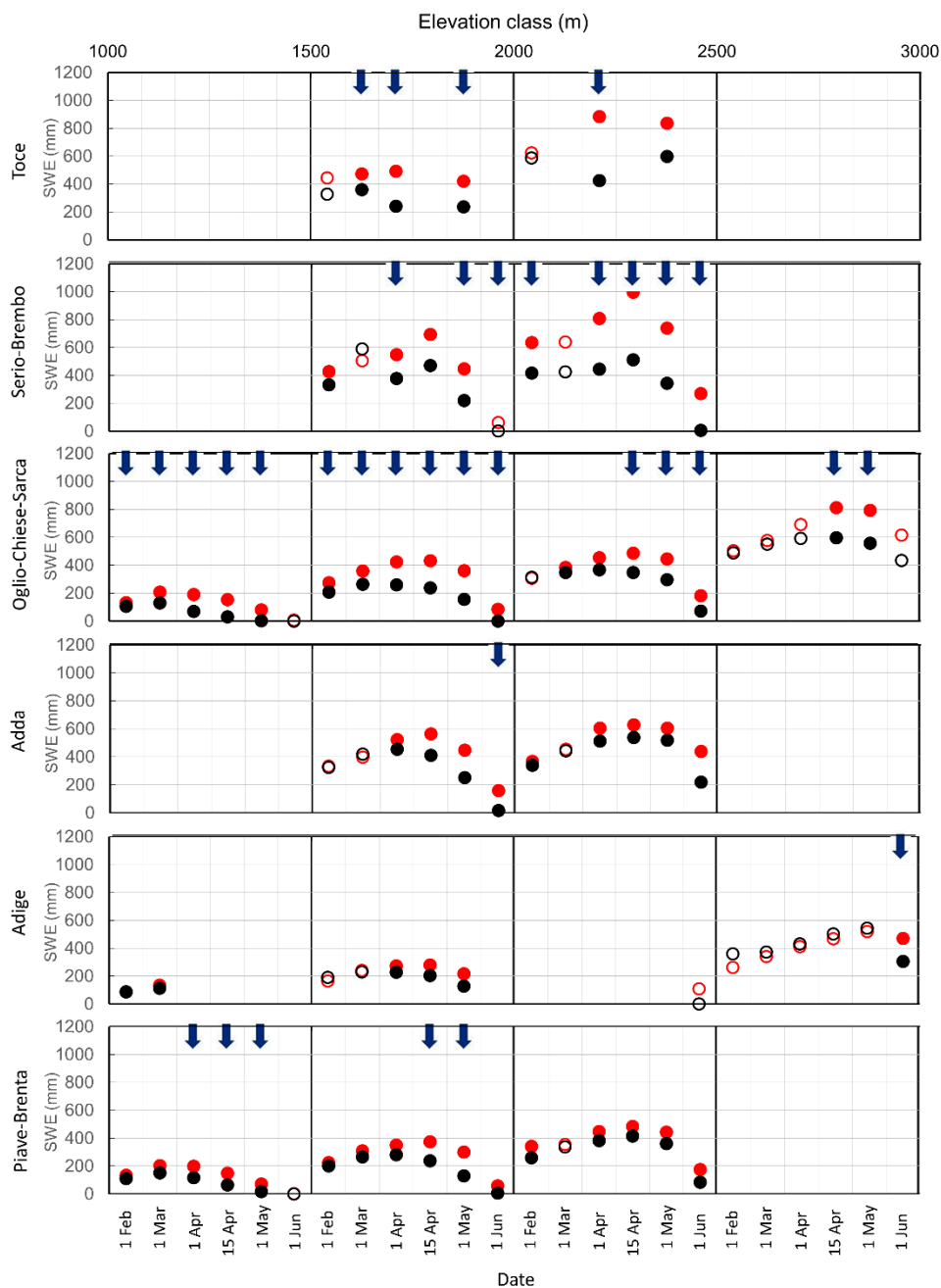


610

Figure 7: Bulk snow density ( $\rho$ ) dependence on elevation for the macro-basin Piave-Brenta. Average snow density for each measurement date is represented with different color intensity with changing date of the year.



615 **Figure 8: Temporal variability of bulk snow density ( $\rho$ ).** Average bulk snow density for each measurement date is represented as black diamond. We also report in red the computed polynomial model, in blue the one proposed in Guyennon et al. (2019) and a linear model as black dashed line.



620 **Figure 9:** Average snow water equivalent (SWE) in the 1967-1993 (red circles) and in 1994-2020 (black circles) periods are plotted  
 for each elevation class in the six observation campaigns dates (1 Feb, 1 Mar, 1 Apr, 15 Apr, 1 May, 1 Jun). Statistically significant  
 ( $p \leq 0.01$ , Mann-Kendall test) trends of the entire 1967-2020 period are sketched as upward (downward) blue arrow for increasing  
 (decreasing) trends. Circles are filled if the difference of SWE between the two periods is statistically significant ( $p \leq 0.01$ , Mann-  
 Whitney test).

625

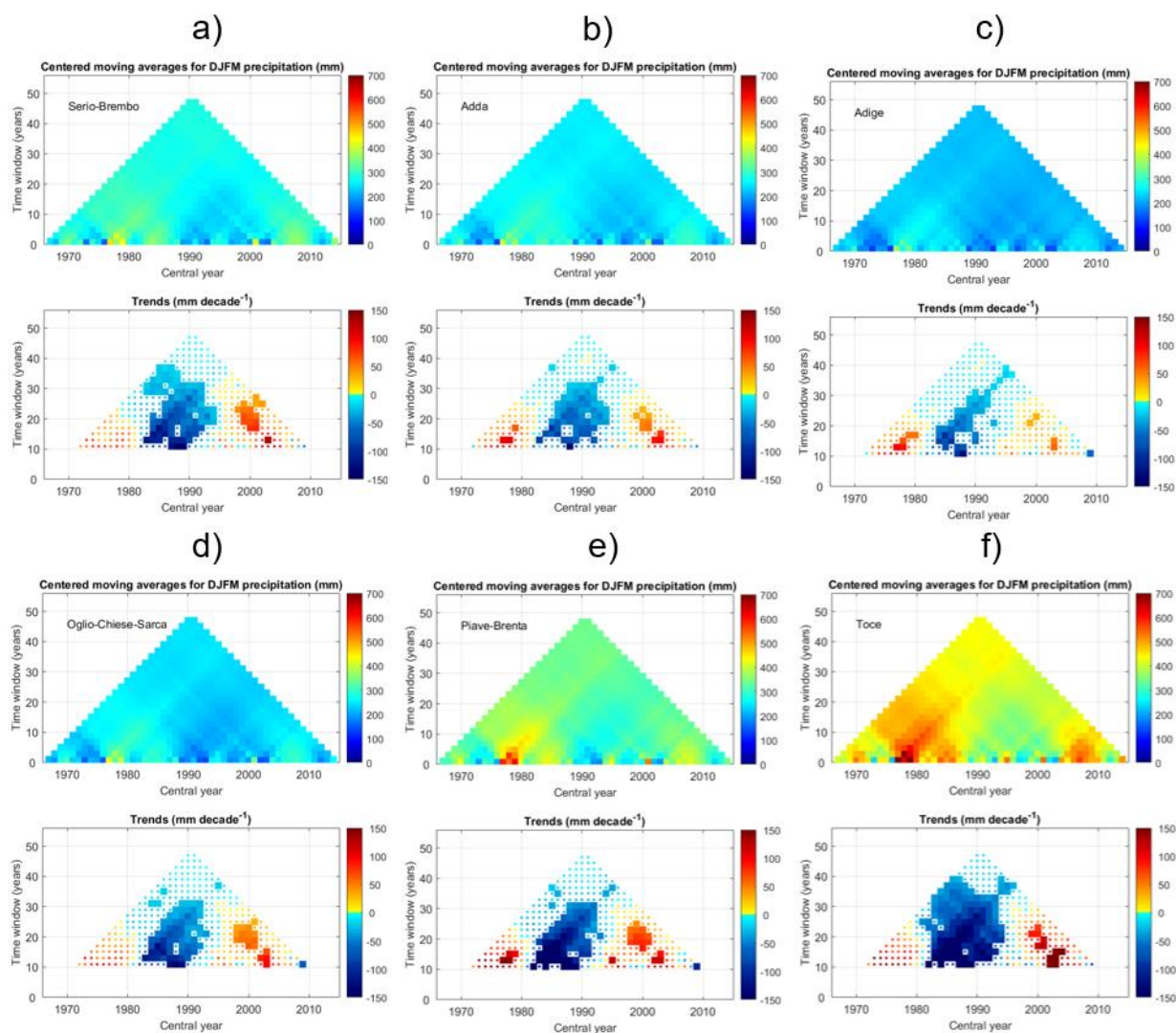
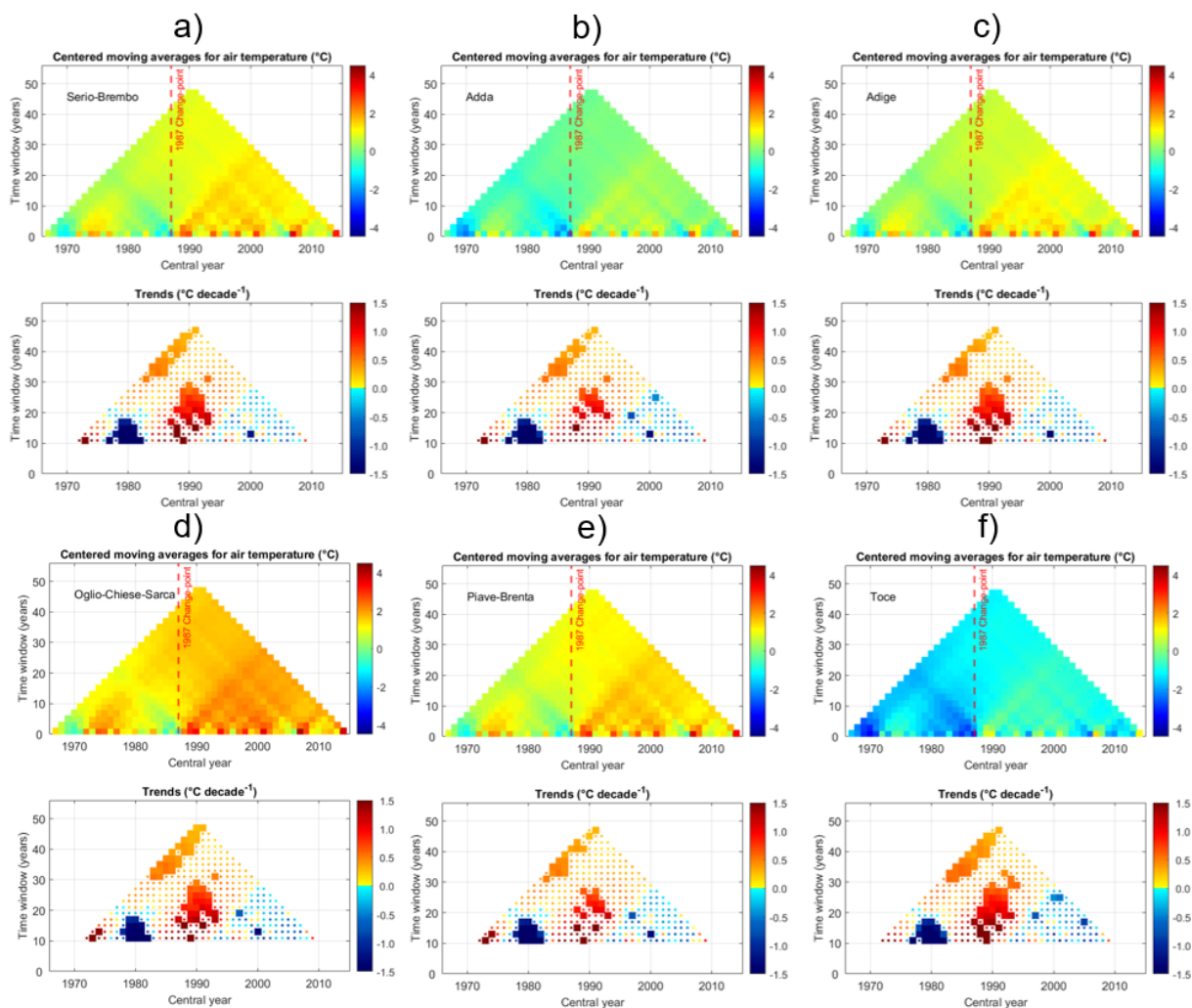
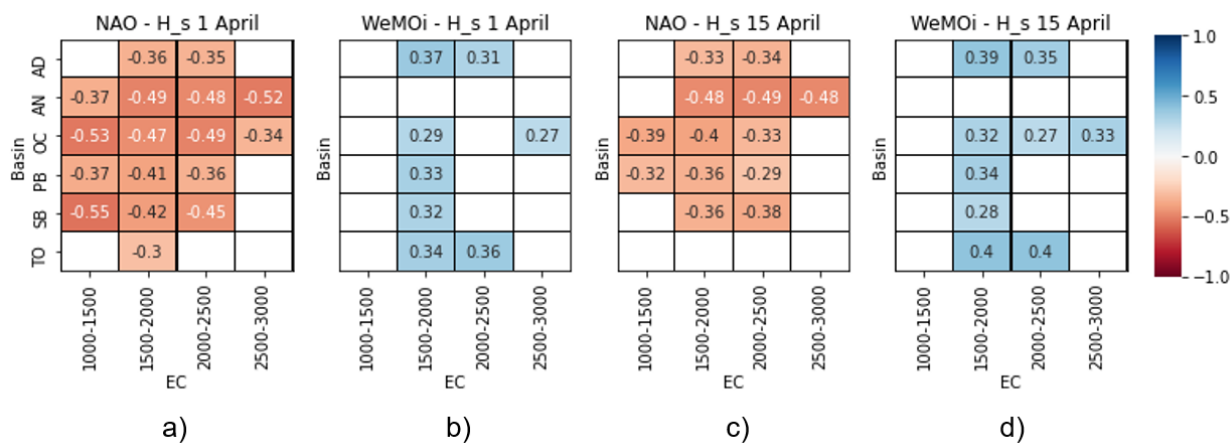


**Figure 10:** MARTA triangles of total winter (DJFM) precipitation for the six macro-basins from the HISTALP dataset. In the bottom part the statistically significant trends with 5% significance level of the Mann – Kendall test are reported as thicker pixels.



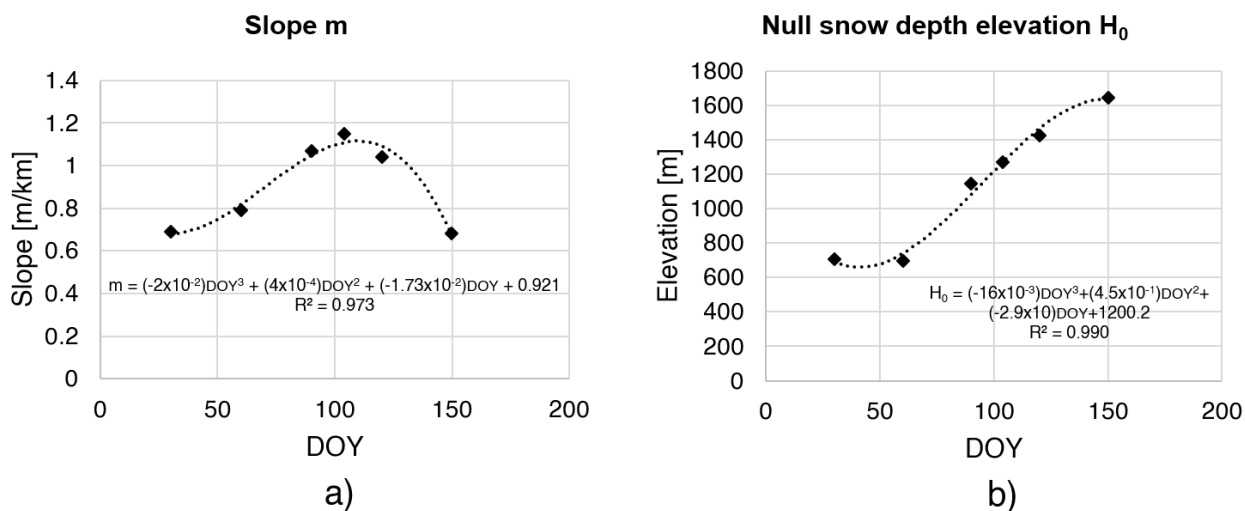
630

**Figure 11: MARTA triangles of average winter (DJFM) temperature for the six macro-basins from the HISTALP dataset. In the top part of each panel the statistically significant change point detected by the Pettitt's test is reported as dashed line while in the bottom part the statistically significant trends with 5% significance level of the Mann – Kendall test are reported as thicker pixels.**



635

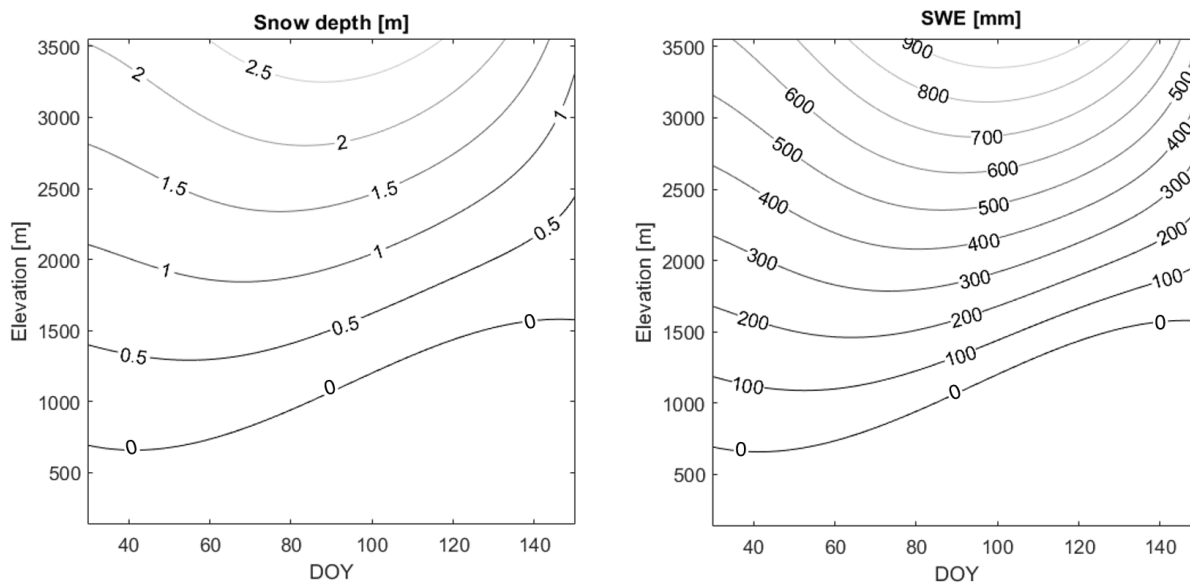
**Figure 12: Statistically significant ( $p < 0.05$ ) Pearson's correlation between winter average teleconnection indexes NAO (a and c) and WeMO (b and d) and the snow depth measured on 1 April (a and b) and 15 April (c and d) for the Toce (TO), Serio-Brembo (SB), Piave-Brenta (PB) Oglio-Chiese-Sarca (OC), Adige (AN) and Adda (AD) and for the four elevation classes (EC).**



640

**Figure 13: Slope  $m$  (a) and null snow depth elevation  $H_0$  (b) as function of the day of the year (black diamonds). Dotted black line represents the third-order polynomial fitting curve (Equation 4 and 5).**





645 **Figure 14: Contour plot of snow depth and snow water equivalent (SWE) in the time-elevation (DOY-H) space for the 1994-2020 period.**



EC	Date	Temporal trend (1967-2019) of snow depth (m decade <sup>-1</sup> )					
		Macro-basin					
		Toce	S-B	O-C-S	Adda	Adige	P-B
1000 – 1500	1 Feb	-	-0.08	-0.07	ND	-	-0.04*
	1 Mach	-	-0.07	-0.09	ND	-	-
	1 Apr	-0.12	-0.10	-0.10	ND	-	-0.07
	15 Apr	-0.10	-0.05	-0.10	ND	-	-0.07
	1 May	-0.06*	ND	-0.06	ND	-	-0.04
	1 June	-	-	-	ND	-	-
1500 – 2000	1 Feb	-	-	-	-	-	-
	1 Mach	-0.09	-0.10*	-0.09	-	-	-
	1 Apr	-0.14	-0.18	-0.13	-	-	-
	15 Apr	-0.17	-0.21	-0.15	-0.13	-	-0.12
	1 May	-0.16	-0.18	-0.18	-0.13	-0.07	-0.13
	1 June	-0.06	-0.08	-0.04	-0.06	-0.02*	-0.03*
2000 – 2500	1 Feb	-	-0.18	-	-	-	-0.05*
	1 Mach	-	-0.24	-0.09*	-0.08*	-	-
	1 Apr	-	-0.27	-0.11	-	-	-
	15 Apr	-	-0.31	-0.13	-0.13*	-	-0.10
	1 May	-	-0.29	-0.16	-0.16	-0.07*	-0.09
	1 June	-0.18	-0.24	-0.08	-0.11	-0.04	-
2500 – 3000	1 Feb	ND	ND	-	ND	-	ND
	1 Mach	ND	ND	-	ND	-	ND
	1 Apr	ND	ND	-0.12*	ND	-	ND
	15 Apr	ND	ND	-0.19	ND	-	ND
	1 May	ND	ND	-0.19	ND	-	ND
	1 June	ND	ND	-0.19	ND	-0.17	ND

**Table 1.** Trends of snow depth (1967 – 2019) for each macro-basin, elevation class (EC) and date. Only statistically significant results according to Mann – Kendall and Student’s t tests are reported. If only one test is passed the trend is marked with an asterisk while cases in which there is not enough data are flagged as ND (no data).



EC	Date	Change point (year)					
		Macro-basin					
		Toce	S-B	O-C-S	Adda	Adige	P-B
1000 – 1500	1 Feb	-	1987	1988	ND	-	-
	1 Mach	-	-	1989	ND	-	-
	1 Apr	-	-	1988	ND	-	1988
	15 Apr	-	-	1986	ND	-	1988
	1 May	-	ND	1989	ND	-	1989
	1 June	-	-	-	ND	-	-
1500 – 2000	1 Feb	-	-	-	-	-	-
	1 Mach	1987	-	1989	-	-	1989
	1 Apr	1988	1988	1988	1988	-	1988
	15 Apr	1989	1988	1988	1988	-	1988
	1 May	1986	1986	1989	1986	-	1989
	1 June	1987	1989	1992	1987	-	-
2000 – 2500	1 Feb	-	1986	-	-	-	-
	1 Mach	-	1989	1989	1980	-	-
	1 Apr	1985	1987	1987	1985	-	1988
	15 Apr	-	1987	1989	1986	-	1987
	1 May	-	1989	1992	1986	-	1989
	1 June	1986	1987	1987	1987	-	-
2500 – 3000	1 Feb	ND	ND	-	ND	-	ND
	1 Mach	ND	ND	-	ND	-	ND
	1 Apr	ND	ND	1986	ND	-	ND
	15 Apr	ND	ND	1989	ND	-	ND
	1 May	ND	ND	1990	ND	-	ND
	1 June	ND	ND	1986	ND	1986	ND

**Table 2.** Years of change-point detected by Pettitt’s test in snow depth timeseries for each macro-basin, elevation class (EC) and date. Only statistically significant results are reported while cases in which there is not enough data are flagged as ND (no data).



Basin	Date	1967 - 1993			1994 - 2020		
		m	H <sub>0</sub> [m]	R <sup>2</sup>	m	H <sub>0</sub> [m]	R <sup>2</sup>
Toce	1 Feb	0.95	593	0.007	1.023	718	0.343
	1 Mach	1.24	650	0.011	1.23	742	0.408
	1 Apr	1.74	941	0.04	1.72	1113	0.509
	15 Apr	1.97	1092	0.068	1.93	1241	0.570
	1 May	2.24	1276	0.121	2.19	1427	0.621
	1 June	2.19	1483	0.262	1.57	1571	0.589
Serio Brembo	1 Feb	1.37	909	0.710	0.91	776	0.616
	1 Mach	1.72	957	0.680	0.83	495	0.310
	1 Apr	1.94	1027	0.582	0.94	712	0.430
	15 Apr	2.12	1128	0.743	1.37	1204	0.644
	1 May	2.13	1260	0.708	1.63	1458	0.280
	1 June	1.23	1522	0.466	1.51	1801	0.403
Oglio Chiese Sarca	1 Feb	0.67	375	0.817	0.69	703	0.725
	1 Mach	0.66	26	0.623	0.79	697	0.696
	1 Apr	0.98	638	0.781	1.07	1145	0.745
	15 Apr	1.22	899	0.784	1.15	1269	0.788
	1 May	1.25	1115	0.791	1.04	1425	0.704
	1 June	0.9	1491	0.515	0.68	1643	0.410
Adda	1 Feb	0.27	-2617	0.013	0.78	1.57	0.235
	1 Mach	0.07	-17704	4.00E-04	0.52	-770.71	0.069
	1 Apr	0.03	-59185	3.00E-05	0.78	288.63	0.111
	15 Apr	0.61	-517	0.017	1.18	1003.38	0.215
	1 May	0.65	-25	0.017	1.73	1504.91	0.379
	1 June	1.66	1638	0.133	1.72	1884	0.676
Adige	1 Feb	0.34	-209	0.663	0.54	570	0.465
	1 Mach	0.43	-341	0.633	0.43	-12	0.668
	1 Apr	0.75	643	0.776	0.78	933	0.589
	15 Apr	0.89	886	0.800	0.98	1197	0.907
	1 May	1.16	1298	0.855	1.16	1442	0.862
	1 June	1.09	1692	0.745	0.49	1634	0.530
Piave Brenta	1 Feb	0.51	92	0.528	0.53	385	0.630
	1 Mach	0.67	101	0.567	0.70	424	0.603
	1 Apr	0.94	646	0.814	0.90	840	0.649
	15 Apr	1.24	953	0.850	1.48	1109	0.742
	1 May	1.16	1144	0.859	0.95	1292	0.709
	1 June	0.53	1333	0.373	0.43	1462	0.408

**Table 3.** Linear regression coefficients (m and H<sub>0</sub>) and R<sup>2</sup> of the least-square linear fitting of average snow depth and elevation for the two sub-periods 1967-1993 and 1994-2020.



EC	Date	Temporal trend (1967-2019) of SWE (mm decade <sup>-1</sup> )					
		Macro-basin					
		Toce	S-B	O-C-S	Adda	Adige	P-B
1000 – 1500	1 Feb	ND	ND	-11*	ND	-	-
	1 Mach	ND	ND	-22	ND	-	-
	1 Apr	ND	ND	-34	ND	ND	-
	15 Apr	ND	ND	-36	ND	ND	-22
	1 May	ND	ND	-21	ND	ND	-14
	1 June	ND	ND	-2*	ND	ND	-
1500 – 2000	1 Feb	-	-	-24	-	-	-
	1 Mach	ND	ND	-27*	-	-	-
	1 Apr	-121	-55*	-43	-	-	-
	15 Apr	ND	-	-59	-	-	-37
	1 May	-85*	-69	-67	-	-	-47
	1 June	-24*	-22*	-21	-	ND	-15*
2000 – 2500	1 Feb	-	-78	-	-	ND	-19*
	1 Mach	ND	ND	-	-	ND	-
	1 Apr	-281	-113	-	-	ND	-
	15 Apr	ND	-191	-38	-	ND	-
	1 May	-	-125	-48	-	ND	-23*
	1 June	ND	-92	-30	-	-	-
2500 – 3000	1 Feb	ND	ND	-	ND	-	ND
	1 Mach	ND	ND	-	ND	-	ND
	1 Apr	ND	ND	-	ND	-	ND
	15 Apr	ND	ND	-61	ND	-	ND
	1 May	ND	ND	-67	ND	-	ND
	1 June	ND	ND	-58*	ND	-55	ND

655 **Table 4.** Trends of snow water equivalent (SWE, 1967–2019) for each macro-basin, elevation class (EC) and date. Only statistically significant results according to Mann–Kendall and Student’s t tests are reported. If only one test is passed the trend is marked with an asterisk while cases in which there is not enough data are flagged as ND (no data).



EC	Date	Change point (year)					
		Macro-basin					
		Toce	S-B	O–C–S	Adda	Adige	P–B
1000 – 1500	1 Feb	ND	ND	-	ND	-	-
	1 Mach	ND	ND	-	ND	-	-
	1 Apr	ND	ND	1988	ND	ND	1986
	15 Apr	ND	ND	1988	ND	ND	1988
	1 May	ND	ND	1989	ND	ND	1988
	1 June	ND	ND	-	ND	ND	-
1500 – 2000	1 Feb	-	-	-	-	-	-
	1 Mach	ND	ND	1988	-	-	-
	1 Apr	-	-	1988	-	-	1988
	15 Apr	ND	-	1988	-	-	1988
	1 May	-	1991	1989	-	-	1989
	1 June	-	-	-	-	ND	-
2000 – 2500	1 Feb	-	1986	-	-	ND	-
	1 Mach	ND	ND	-	-	ND	-
	1 Apr	-	1988	1987	-	ND	1988
	15 Apr	ND	-	1988	-	ND	-
	1 May	-	1990	1989	-	ND	1987
	1 June	ND	-	1986	-	-	-
2500 – 3000	1 Feb	ND	ND	-	ND	-	ND
	1 Mach	ND	ND	-	ND	-	ND
	1 Apr	ND	ND	1986	ND	-	ND
	15 Apr	ND	ND	1986	ND	-	ND
	1 May	ND	ND	1986	ND	-	ND
	1 June	ND	ND	1986	ND	-	ND

**Table 5.** Years of change-point detected by Pettitt’s test in SWE timeseries for each macro-basin, elevation class (EC) and date. Statistically significant results only are reported while cases in which there is not enough data are flagged as ND (no data).